Silica Scaling in Closed-Circuit Desalination (CCD)

Master Thesis

Thayn Malar Motchan

Technische Universiteit Delft

TU Delft Delft University of Technology

Challenge the future

Silica Scaling in Closed-Circuit Desalination

by

Thayn Malar Motchan

in partial fulfilment of the requirements for obtaining the degree of

Master of Science in Civil Engineering

at Delft University of Technology

Thesis Committee:

Dr. ir. S. G. J. Heijman (chair)	Delft University of Technology
Dr. ir. A. H. Haidari	Delft University of Technology
Prof. dr. E. J. R. Sudhölter	Delft University of Technology
Dr. ir. H. Spanjers	Delft University of Technology

January 2019

TUDelft

Preface

This report concludes my master thesis for the MSc Water Management program, specialising in Sanitary Engineering, at Delft University of Technology. My research was based on substantial laboratory work in the Water Lab of TU Delft. Although the work was challenging, it was well worth the knowledge and experience I gained in the process.

Firstly, I would like to thank my supervisors, Bas Heijman and Amir Haidari for guiding and advising me throughout my research work. I also thank the other members of my thesis committee, Ernst Sudhölter and Henri Spanjers for supporting me by providing timely and invaluable feedback.

I am very grateful for the help I received in the laboratory, especially while building my setup. Thank you, Mohammed Jafar and Armand Middeldorp, the Water Lab technicians, for being ever ready to help and assist me whenever needed. I also thank Sander de Vree and Frank Kalkman, from the Fluid Mechanics Laboratory, for helping me set up my data logging system. Thank you, Léon Roessen from DEMO, for assisting me when my setup required specific fittings.

My colleagues who worked in the lab with me, thank you for providing ideas and solutions when I faced hurdles with my setup. We shared a good camaraderie and an enjoyable experience working together in the lab.

I would like to thank my family for providing unwavering support and motivation throughout my study. Their support enabled me to overcome the challenges I faced in this research. I end by thanking my friends from Water Management and Environmental Engineering for always being there for me and for making my study in Delft a memorable time.

Thayn Malar Motchan

Delft, January 2019

Abstract

With the growing population and industrial development, there is more stress on natural water resources. Additionally, environmental laws make the disposal of waste streams from industries difficult. In this scenario, it is crucial to treat waste streams to recover water and possibly minerals, for reuse in the industry, reducing the dependency on new resources. Reverse osmosis (RO) is a membrane-filtration technology that has been in use for decades. RO systems can waste up to 30% of the feed water through the production of brine, containing the rejected minerals. This rejection is high when dealing with saline waters. Treatment of this brine stream for reclamation of water would increase the overall efficiency of RO systems. In this research, the treatment of RO brine by a closed-circuit configuration of RO – closed-circuit desalination (CCD) - is investigated. In CCD, filtration is done in batches, with the recirculation of the concentrate stream back into the feed stream. The high cross-flow velocity and short filtration batches result in prevention of scaling in these systems.

This research focused on proving the resilience of the CCD system to silica scaling despite supersaturations of silica. Lab-scale experiments were performed on a single-element CCD system, specially built with relevant measurement instruments. Silica scaling was monitored by mass transfer coefficient (MTC) calculations, silica mass balance calculations, and membrane autopsies. Synthetic feed water was used, containing only NaCl (10 mg/L) and varying concentrations of silica (70 – 120 mg/L as SiO_2). No anti-scalants were used. Longer experiments were performed, i.e. 20 consecutive cycles of 1 hour each with 120 mg/L of silica in the feed. The cycle duration was increased, 2 cycles of 3-hour each were performed, with 120 mg/L of silica in the feed.

The MTC curves in all the experiments had a gradual decline with the progression of each cycle, but always recovered at the beginning of the next cycle. This decline was probably due to the increasing osmotic pressure in the recirculation loop. There was no permanent decline in the MTC, leading to the observation that there was no scaling in the system. This was supported by the silica in the mass balance calculations, that showed there was no loss of silica from the brine. The reactive silica concentration in the brine was as high as 1800 mg/L in the 3-hour cycle, attaining a recovery of 93%, without signs of scaling. The membrane autopsy showed that the membranes used for the experiments with 120mg/l silica in the feed had higher silicon content compared to the blanks. However, there were too few samples to compare against and make strong conclusions whether there was scaling.

Thus, the designed CCD system was resistant to silica scaling in these conditions, of high pH and in the absence of other components such as iron, aluminium, calcium and magnesium. The results of this study proved that, despite high concentrations of silica in the feed, CCD can improve the total efficiency of RO systems (with regard to the water wastage) by recovering water from the brine produced by RO installations. The extremely high recoveries attained by the system would result in small volumes of very concentrated brine, making the extraction of minerals more cost-effective, because lesser volumes must be treated to obtain the same amount of minerals.

Contents

List of Figures

List of Tables

Chapter 1

Introduction

1.1. General Overview

Reverse osmosis (RO) is an important treatment step for water production and water recovery. RO was first commercialised in the 1970s [1] and has broad applications in the fields such as drinking water production, pharmaceuticals, food and beverage industries, to name a few [2]. RO installations produce clean water along with the constant production of a brine stream, containing all the rejected minerals. The system recovery of a RO installation represents the percentage of clean water produced by the installation from the total feed water consumed. This consequently dictates the volume of brine produced by the system. In general, majority of RO systems are designed for a system recovery of about 75%, resulting in wastage of 25% of the feed water through brine flow [3]. This percentage wastage can be much higher when treating highly-saline feed sources, as an example [1].

The strain on water resources would increase with the predicted growth in global population. Additionally, growth in the gross domestic product (GDP) has resulted in increase in the industrial water use [4]. Thus, water resources, especially fresh water resources, need to be used efficiently, increasing the importance of alternate sources of water for the industry. Since 2002, there has been a 40% increase in the use of RO systems for treatment of river water. RO application is predicted to increase world-wide, with industrial growth and tighter environmental regulations [2], thus enhancing the need for treatment solutions for the produced brine streams. The brine produced in RO systems contain all the minerals rejected from the feed water. Depending on the type of feed water and the recovery, these streams can be quite saline. The discharge of the more saline brine streams can be quite problematic, with environmental fees imposed on discharge into rivers, for example. Thus, it would be beneficial to treat these streams for the reclamation of water and possible extraction of minerals.

The ZERO BRINE Project (*European Union's Horizon 2020 Research and Innovation Programme*) is targeted at the reclamation and reuse of minerals and water from waste streams of industrial processes. One of the cases of this project is the *EVIDES* demineralised water

production plant in the Botlek area. At this plant, demineralised water is produced from a surface water source, with RO as one of the treatment steps. The ZERO BRINE project aims to treat the brine produced by this RO installation to recover water and minerals from the stream. [5]

Table 1. Composition of the RO brine from the EVIDES demineralised water production plant (ZERO BRINE).

Component	Concentration (mg/L)
Sodium (Na^+)	1000
Bicarbonate (HCO_3^-)	1067
Chloride (Cl^-)	600
Silica (H_4SiO_4)	52 (32.5 mg/L as SiO_2)
Sulphate (SO_4^{2-})	387
Total Organic Carbon (TOC)	16.5

Table 1 shows the composition of the brine stream. A treatment technology is required to separate as much water from this stream, producing an even more concentrated brine stream, from which extraction of minerals would be possible. Achieving high recoveries in this step is crucial to reclaim as much water as possible, while producing small quantities of brine. Lesser volumes of brine result in more cost-effective extraction of minerals, because less water must be treated to obtain the same amount of minerals.

With permeate production in RO systems, the concentration of dissolved compounds on the feed side of the membrane increases. The concentration factor is related to the recovery of the system. For a specific feed water, higher recovery results in higher concentrations of these compounds in the system, especially in the last element of the RO installation. Sparingly-soluble compounds may precipitate on the membrane at supersaturated concentrations, forming scale. With scaling, the energy consumption of filtration increases, because more energy is needed to maintain a constant flux. Additionally, more frequent chemical cleaning is required, decreasing the life expectancy of the membrane. [6]

Hence, the safe recovery achievable by RO systems is restricted by certain components in the feed water. Silica is one such component. As the recovery is increased, the concentration of silica in the brine is also higher, increasing the risk of scaling. Silica scaling on the membrane is difficult to remove and could permanently damage the membrane. In practice, silica scaling in RO systems is prevented by maintaining concentrations lower than 150 mg/L, at temperatures above 21°C [7]. With the use of anti-scalants, the safe level of silica concentration is increased to 300 mg/L [8].

The brine stream from the RO system in the *EVIDES* plant has a high concentration of silica (as seen in Table 1).[1] Hence, the goal of achieving high recoveries of water from the RO brine might be hampered by the silica concentration in the brine. To attain this goal, a closed-circuit configuration of RO – closed-circuit desalination (CCD) - is considered, wherein filtration is done in batches, with the recirculation of the concentrate stream back into the feed stream.

[1] *Natural waters typically contain 1 to 40 mg/L of silica (as SiO_2)* [8] [18].

CCD has many benefits when compared to conventional RO systems. CCD systems have much lower energy consumption as the concentrate recycling results in prevention of energy loss in the brine stream. Constant recirculation of the brine reduces membrane fouling, thereby minimising membrane cleaning costs. Moreover, membrane performance is improved in CCD. [9] [10] Stover compared the recovery of conventional RO and closed-circuit RO, using feed water containing a silica concentration of 59 mg/L. The recovery of the conventional RO was limited to 76%; the closed-circuit RO however, attained 93.5% recovery, while generating a brine stream with 900 mg/L of silica [1].

Thus, in this research, CCD is explored as an option for the treatment of RO brine for the reclamation of water. With CCD, it would be possible to reduce the brine to very high concentrations, thereby recovering a large portion of water. Hence, the effectiveness of CCD in preventing silica scaling during filtration is investigated in this project.

Research shows that batch RO can concentrate RO brine streams due to the resistance to inorganic fouling when compared to conventional RO [11]. Several studies have proven that batch RO can tolerate silica concentrates much higher than solubility levels. Brine silica concentrations as high as 700 mg/L were achieved from feed water containing 125 mg/L of SiO_2 and 10,000 mg/L of NaCl [12]. However, these results were based on model simulations and not experimental work. Pilot-plant experiments with batch RO succeeded in concentrating the brine from a desalination plant, reaching concentrations of over 1000 mg/L SiO_2 in the concentrate [13]. This was achieved with pH control (< 4.5) and the use of anti-scalants (for $CaSO_4$ and silica). The addition of anti-scalants increases the threshold beyond which scaling would occur. However, it also results in the introduction of more components into the waste stream, further complicating mineral extraction, and so, will be avoided in this study.

There is a need for experimental work to prove the resistance of fouling in CCD systems with supersaturations of silica in the concentrate, without the use of anti-scalants. This should include accurately monitoring silica scaling during filtration. Apart from this, it would be beneficial to understand the effect of parameters such as cycle duration and initial feed salinity on the occurrence of silica scaling in the system. Such experimental work would be the beginning of the development of a solution for managing brine produced by RO plants with silica in the source water.

1.2. Objectives

This study evaluates the effectiveness of closed-circuit desalination (CCD) in delaying, reducing, or even preventing silica scaling on RO membranes when dealing with feed containing significant levels of silica. The objectives of this thesis are:

- To design and build a CCD setup, with meters to monitor relevant parameters
- To accurately monitor silica scaling in the CCD setup via,
    - Continuous measurements of mass transfer coefficient (MTC)
    - Mass balance calculations of silica (SiO_2) in the system
    - Destructive analysis of the membrane (autopsy and microscope)
- To assess the effect of *longer experiments* (more consecutive cycles) on the occurrence of silica scaling in the system
- To assess the effect of *longer cycle duration* on the occurrence of silica scaling in the system

Chapter 2

Background

2.1. Closed-Circuit Desalination (CCD) vs. conventional Reverse Osmosis (RO)

Reverse osmosis (RO) is a membrane filtration process that can remove almost all dissolved matter from the feed. It can remove metal ions, dissolved salts and even viruses [14]. Osmotic flow occurs when water flows through a membrane from a diluted solution to the concentrated solution. Reverse osmosis is based on applying pressure on the feed side to push water through the membrane, against the natural osmotic flow. The applied pressure must be greater than the osmotic pressure difference across the membrane. The efficiency of this technology is susceptible to fouling, both inorganic and biological, with surface fouling being the main fouling mechanism [15]. Figure 1 shows the schematics of a basic RO system. Q_f, Q_p and Q_b are the feed, permeate and brine flow rates respectively; FP is the feed pump.

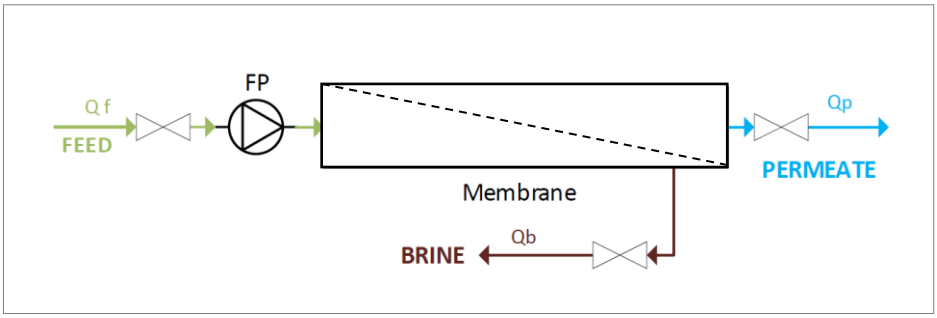

Figure 1. Schematics of a conventional RO setup.

Closed-circuit desalination (CCD) operates on the same principle as reverse osmosis, but in a different configuration. CCD involves a batch operation, in contrast to the continuous operation of conventional RO. CCD involves circulation of the concentrate stream. Figure 2 is an illustration of the CCD system. $Q_{f,fresh}$ and Q_c are the fresh feed and recirculated concentrate flow rates, respectively; CP is the circulation pump.

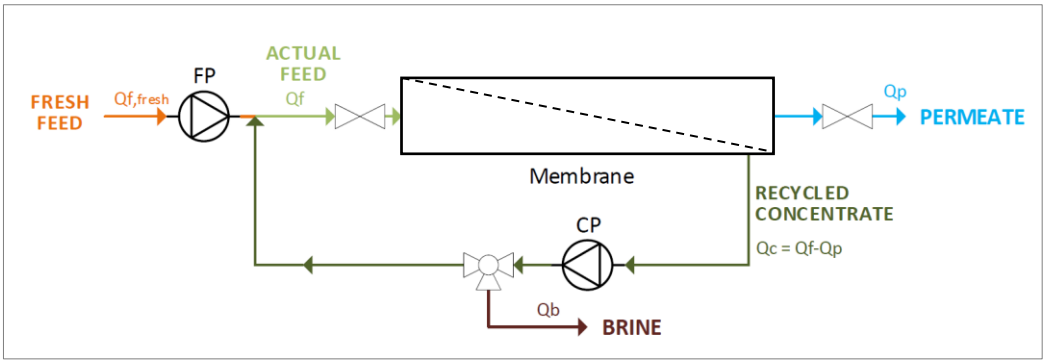

Figure 2. Schematics of closed-circuit desalination (CCD) setup.

CCD is run in cycles, during which there is no brine discharge. All the concentrate produced is mixed with incoming fresh feed and then fed into the membrane module again. At the end of the cycle, the spent concentrate is discharged and replaced with fresh feed. The components of CCD are a feed pump, a circulation pump and a 3-way valve for brine discharge.

By circulation of the concentrate in a CCD system, a cross-flow is created over the membrane surface. This cross-flow reduces concentration polarisation at the membrane surface, by disturbing the boundary layer formed [14]. This greatly reduces fouling and scaling of the membrane, allowing much higher recoveries. If the concentrate recirculation in CCD was stopped, concentration polarisation would increase and consequently, the flux through the membrane would stop [10].

In RO systems, there is a significant loss of energy through the concentrate stream. In CCD systems, the concentrate stream is recirculated back into the feed. This reduces the volume of fresh feed let into the system, thereby reducing the volume of water to be pressurised by the feed pump. In a CCD setup, the pressure is varied through the cycle, to maintain a constant fresh feed flow. Hence, the pressure does not remain at the maximum level through the cycle, unlike RO systems. The pressure is gradually increased and is at maximum only towards the end of each cycle. Thus, there are significant energy savings in CCD systems compared to conventional RO systems [10] [9].

CCD is performed in cycles of a fixed duration, under variable feed pressure to maintain a fixed fresh feed flow. The volume of permeate produced in a single cycle can be expressed with Equation 2.1. As the volume of the system is constant, and the brine flow (wastage) is zero, the feed flow rate is equal to the permeate flow rate. The system volume is the capacity of the pipes and vessels that the system is comprised of. The system recovery in CCD can be calculated based on the volume of permeate produced and system volume, equation 2.2.

$$V_p = Q_{f,fresh} \cdot t_{cycle} = Q_p \cdot t_{cycle} \tag{2.1}$$

$$\gamma_{sys} = \frac{V_p}{V_p + V_{sys}} \cdot 100 \tag{2.2}$$

Where,

V_p is the volume of permeate produced in L;

$Q_{f,fresh}, Q_p$ are the flow rates of the fresh feed and permeate, respectively, in L/h;

t_{cycle} is the cycle duration in *h*;

V_{sys} is the system volume in *L*; and

γ_{sys} is the system recovery as a percentage.

Using Equations (2.1) and (2.2), the relation between cycle duration and system recovery is expressed using Equation 2.3. As V_{sys} and Q_p are constant during a cycle, γ_{sys} is a function of t_{cycle} [10].

$$t_{cycle} = \frac{\gamma_{sys} \cdot V_{sys}}{Q_p \cdot (100 - \gamma_{sys})} \tag{2.3}$$

In conventional RO systems, the feed, permeate and concentrate quality remain constant during operation. In CCD, with more recovery during each cycle, the salinity in the recirculation loop increases, resulting in increasing salinity of the permeate, as the cycle progresses [16]. Higher salinity in the recirculation loop results in higher osmotic pressure as each cycle progresses. This means the pressure applied by the feed pump needs to be gradually increased to supply the required driving force to keep the flux constant.

2.2. Silica Chemistry

Silica, the main component of the Earth's crust, exists in our environment in combination with oxides of magnesium, aluminium, calcium and iron. It occurs in natural waters as a result of weathering of silicate minerals in the rocks and soil, usually at concentrations of 1 to 40 mg/L [8] [18].

2.2.1. Forms of Silica

Monomeric silica (H_4SiO_4) is the soluble form of silica at pH below 9. It is also called silicic acid, monosilicic acid, reactive silica, soluble silica and hydrated SiO_2. Monomeric silica undergoes polymerisation in super-saturated solutions. Polymeric silica first grows linearly with three or four silica units and then adopts a cyclic structure. In time, the polymers form internal cross-links and continue growing by the addition of monomers. The surface of the polymer will have many silanol groups (≡Si-OH) compared to the bulk. These silanol groups on the polymer surface undergo ionisation at pH greater than 7, resulting in the negative charge of silica polymers. Polymers of size between 0.001 µm to 1 µm are referred to as colloidal silica (as per the IUPAC classification). These colloids are stable in solution but can also precipitate in the presence of polyvalent metal ions. [8] The main factors affecting the solubility of silica are temperature, pH, presence of metal ions, co-precipitation, ionic strength, and time [19].

2.2.2. Mechanisms of Scaling

There are two mechanisms for silica scaling, i.e. polymerisation of monomers forming amorphous silica deposits, and heterogenous nucleation of monomers in the presence certain components [8].

2.2.2.1. Polymerisation of monomers

The rate of polymerisation of monomeric silica is fastest at a pH of 6 to 8 [7] [20]. Monomeric silica is very stable; however, once polymerisation starts - even a small amount - the monomers are very quickly polymerised. Colloidal silica can clog the feed channel spacer and foul the membrane. Higher initial concentrations increase the rate of polymerisation. The silica polymers can form scale precipitates through reaction with even trace amounts of polyvalent metal ions, i.e. aluminium or iron [8].

At high pH, around 9, there is an increase in silica solubility and decrease in silica polymerisation. With this, the potential for the formation of highly-insoluble calcium-magnesium silicates increases. Figure 3 shows the relation between the polymerisation rate and the pH for a solution of 550 mg/L of SiO_2, at 50°C [7].

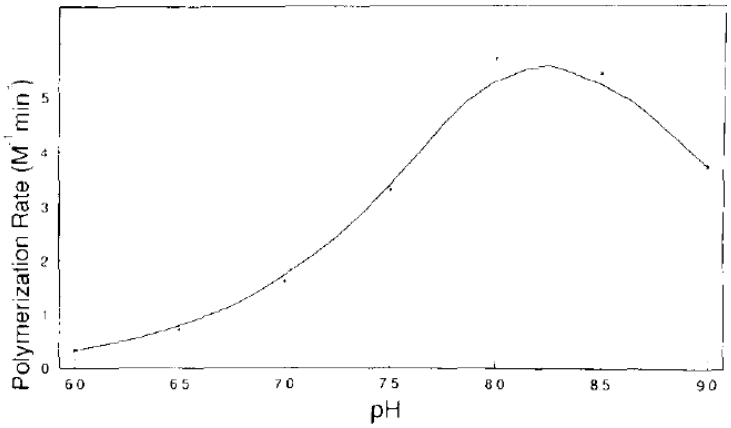

Figure 3. Rate of polymerisation of silica (550 mg/L SiO_2, 50°C) [7].

2.2.2.2. Heterogenous nucleation of monomers

Apart from polymerisation, silica scale can be formed through heterogenous nucleation of silica monomers with non-silica colloids, pre-existing scale or corrosion products. This can result in the formation of a glassy, impermeable layer on the surface of the membrane [8].

2.3. Delay of scaling in CCD systems

In continuous RO systems, supersaturated conditions are reached almost immediately due to build-up of a layer of retained material close to the membrane surface, and this state is maintained until mechanical cleaning. To reduce the effects of concentration polarisation, the cross-flow velocity can be increased, by increasing the feed flow velocity in the membrane module. However, this also changes the permeate flux and the recovery of the system. In CCD, the cross-flow can be adjusted without affecting the flux and recovery, due to concentrate recycling.

2.3.1. Concentration Polarisation

During membrane filtration, there is a build-up of a layer of retained ions, close to the membrane surface. This phenomenon is called concentration polarisation, represented in Figure 4.

Concentration polarisation results in an initial rapid decline of flux. The osmotic pressure in the boundary layer rises with concentration polarisation, causing a higher difference in the osmotic pressures across the membrane [14]. This layer results in higher initial feed pressure to overcome the osmotic pressure difference at the boundary layer and push the water through the membrane.

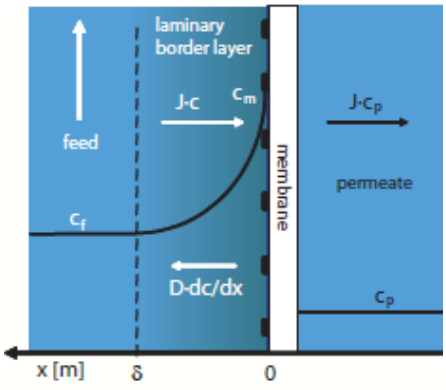

Figure 4. Concentration polarisation. [14]

The effects of concentration polarisation can be reduced by generating turbulence along the membrane surface that disturbs the boundary layer formed. In conventional RO, turbulence is created by using spacers, or by increasing the feed flow velocity in the membrane module [17] [14]. In CCD, circulation of the concentrate flow back into the membrane module maintains the cross-flow required to limit concentration polarisation [10].

2.3.2. Salinity Cycling

In the study done by Warsinger et al., the occurrence of inorganic fouling was predicted by comparing the system residence time to the nucleation induction time for salt crystals [11]. The nucleation induction time (t_{ind}) is defined as the time taken for the formation of stable crystals in a solution in the supersaturated state. The system residence time (t_{res}) is defined as the duration in which highly supersaturated parts of the feed solution are present in the module. Crystallization is predicted to occur when the residence time approaches induction time. Hence, scaling can be prevented if the residence time is kept lower than the induction time ($t_{res} < t_{ind}$).

In CCD systems, the operation is run in cycles. In each cycle, the concentration of the feed solution in contact with the membrane varies. Figure 5 depicts the salinity in the last membrane element in CCD and continuous RO [11]. The concentration of the foulant in the feed gradually increases until the end of the cycle when it drops again when the brine is discharged, and fresh feed introduced. In conventional RO, the final element is in contact with super-saturated feed solution throughout the process. Thus, in CCD, the duration of exposure of the membrane to super-saturated feed is greatly reduced compared to conventional RO, i.e. the system residence time is much smaller [11]. Hence, silica scaling in the final membrane element is delayed in CCD systems compared to continuous RO systems.

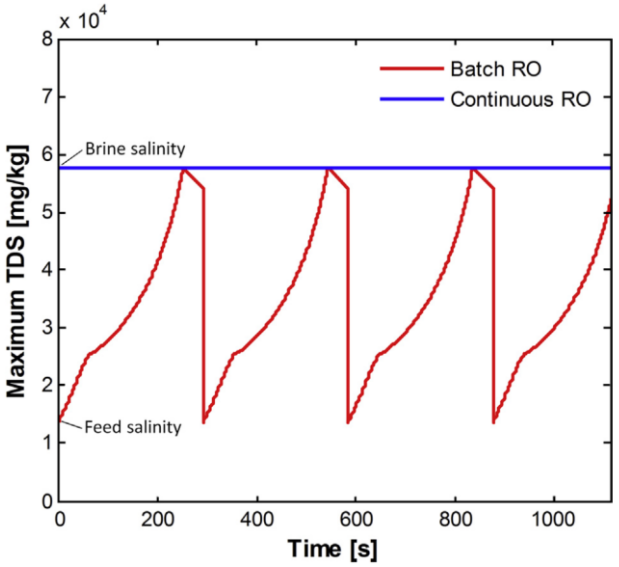

Figure 5. Salinity in the last membrane element in CCD vs. continuous RO [11].

Despite CCD being able to concentrate feed containing foulants such as silica past saturation levels, when the feed is supersaturated at the start of the cycle in CCD, fouling is observed [12]. Thus, in practice, it is important that the feed be below saturation levels at the start of each cycle.

2.4. Mass Transfer Coefficient (MTC)

In practice, scaling on the membrane surface is detected by measuring the mass transfer coefficient (MTC) [6] [21]. When scaling occurs, there will be a decrease in the MTC. Hence, scaling is expressed in terms of the rate of decrease of MTC. The acceptable rate of decline in MTC depends on several factors such as economics (i.e. it is not fixed). In the study done by Heijman et al., MTC was calculated continuously by measuring the feed flow, feed pressure, feed temperature, feed conductivity, the pressure-drop across the membrane, and the permeate flow [21].

In their study, Lisdonk et al. have concluded that MTC is independent of the flux. When the flux was tripled, there was a decrease in the MTC, and a 4% decrease in the calculated concentration polarisation. The decrease in MTC was attributed to entrance flow losses with increased flow [6].

Chapter 3

Materials and Methods

3.1. Feed water

Model feed water was used for the experiments. The model feed water was prepared by dissolving sodium trisilicate solution [22] in demineralised water (electrical conductivity (EC) lower than 10 µS/cm) to achieve the required SiO_2 concentration.

The high solubility and rejection of NaCl make it ideal to use to calculate the concentration factor of the system. The concentration of Na could be determined from the EC of the solution. The variation of EC of a solution with increasing concentrations of NaCl was modelled using PHREEQC [23]. Figure 6 shows the results of the modelling. It is evident that the relation between the EC of the solution and the concentration of NaCl is linear.

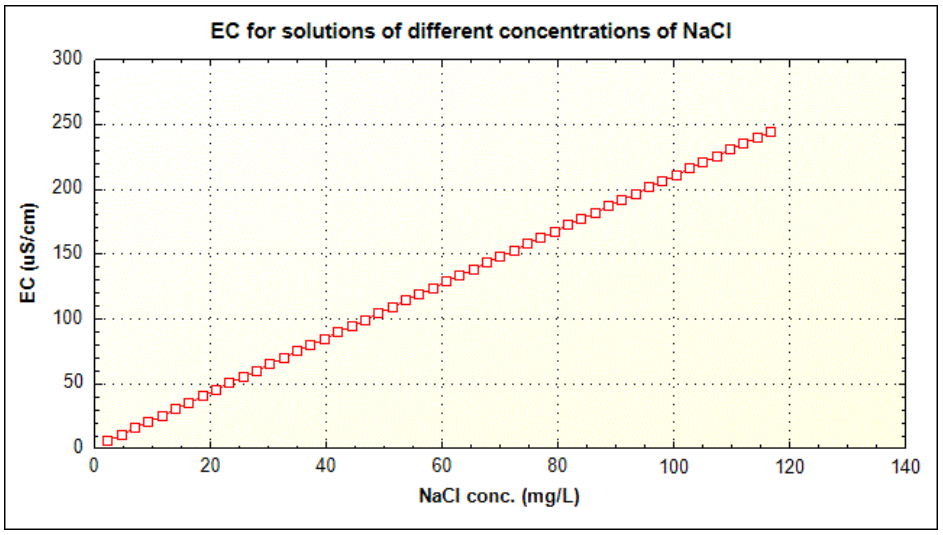

Figure 6. EC of solutions with varying concentrations of NaCl.

The effect of SiO_2 on the EC of a solution was investigated by similar PHREEQC modelling, calculating the EC of solutions containing 10 mg/L of NaCl and increasing concentrations of

SiO_2. Figure 7 shows the results of the modelling. As seen clearly, increasing the silica concentrations does not affect the EC of the solution, compared to the effect of increasing NaCl. Thus, the EC measurements made in the system would be representative of the sodium concentration in the brine.

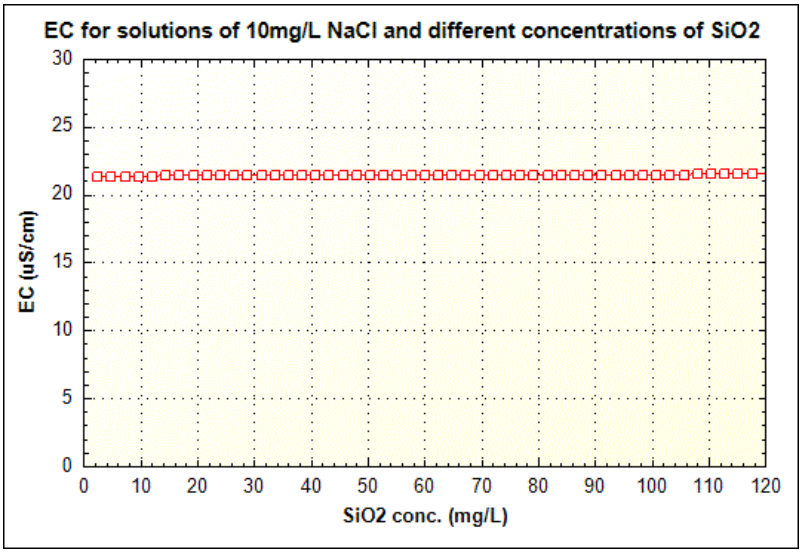

Figure 7. EC of a solution of 10 mg/L NaCl and varying concentrations of SiO_2.

Hence, the expected SiO_2 concentration was determined using the concentration factor calculated from the EC measurements, and then compared to the measured SiO_2 in the brine. If scaling occurred, there would be a difference in the expected and measured values of SiO_2. A low concentration of NaCl is vital to keep the osmotic pressure in the feed low. Thus, the feed solution was prepared with 10 mg/L of NaCl.

Initially, a concentration of 35 mg/L SiO_2 in the feed was used, based on the SiO_2 values in the brine produced in the RO installation in a demineralised water production plant (ZERO BRINE Project Report). In the subsequent experiments, 70, 80 and 120 mg/L SiO_2 were used. The concentration of NaCl added to the feed was kept constant at 10 mg/L.

Figure 8 shows change in pH with varying concentrations of silica with 10 mg/L NaCl. The pH of the feed remained constant at about 10.

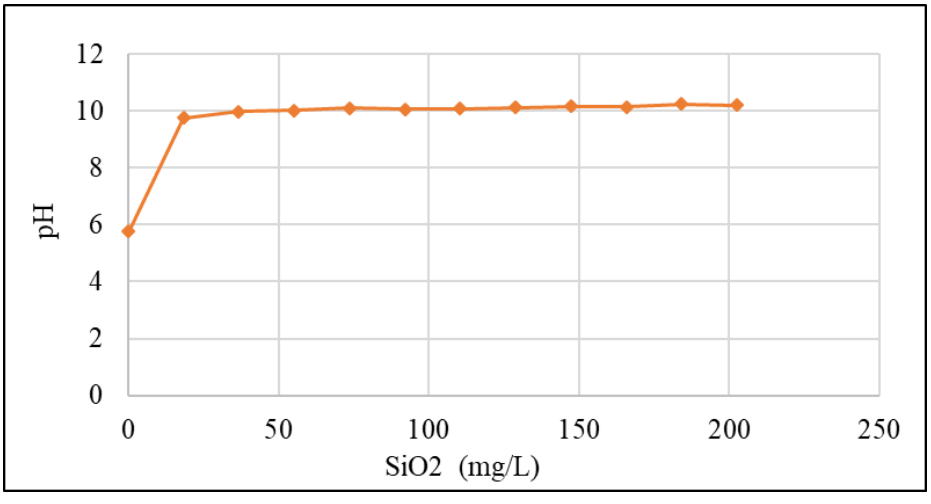

Figure 8. pH for different concentrations of silica with 10 mg/L NaCl.

The feed water was prepared in batches, in 10-litre plastic jerry tanks. The sodium trisilicate solution and NaCl for each tank was measured separately on an electrical balance, to an accuracy of 0.1 mg. The measured solution and salt were dissolved in demineralised water, which was measured with an electric balance to ensure accuracy. The EC of each tank was measured to ensure uniform quality of the prepared feed.

3.2. Experimental Setup and Operation

3.2.1. Description of the CCD setup

In the CCD system, during each cycle, the concentrate stream was recirculated back to the feed, and through the pressure vessel continuously. Recirculation was done without any wastage of the concentrate stream during the batch operation, i.e. $Q_b = 0$ during a cycle. At the end of each cycle, the concentrated feed in the loop (i.e. the brine) was discharged. At the same time, fresh feed was pumped into the loop, flushing out the brine.

Due to concentrate recirculation, the stream that entered the membrane module, the actual feed (Q_f), was not equal to the fresh feed stream ($Q_{f,fresh}$). Hence, for CCD, the actual feed flow was the fresh feed flow ($Q_{f,fresh}$) mixed with recycled concentrate (Q_c), i.e. Q_f. Hence, the measurements for the calculation of MTC had to be performed on this stream. Figure 9 shows the CCD setup built.

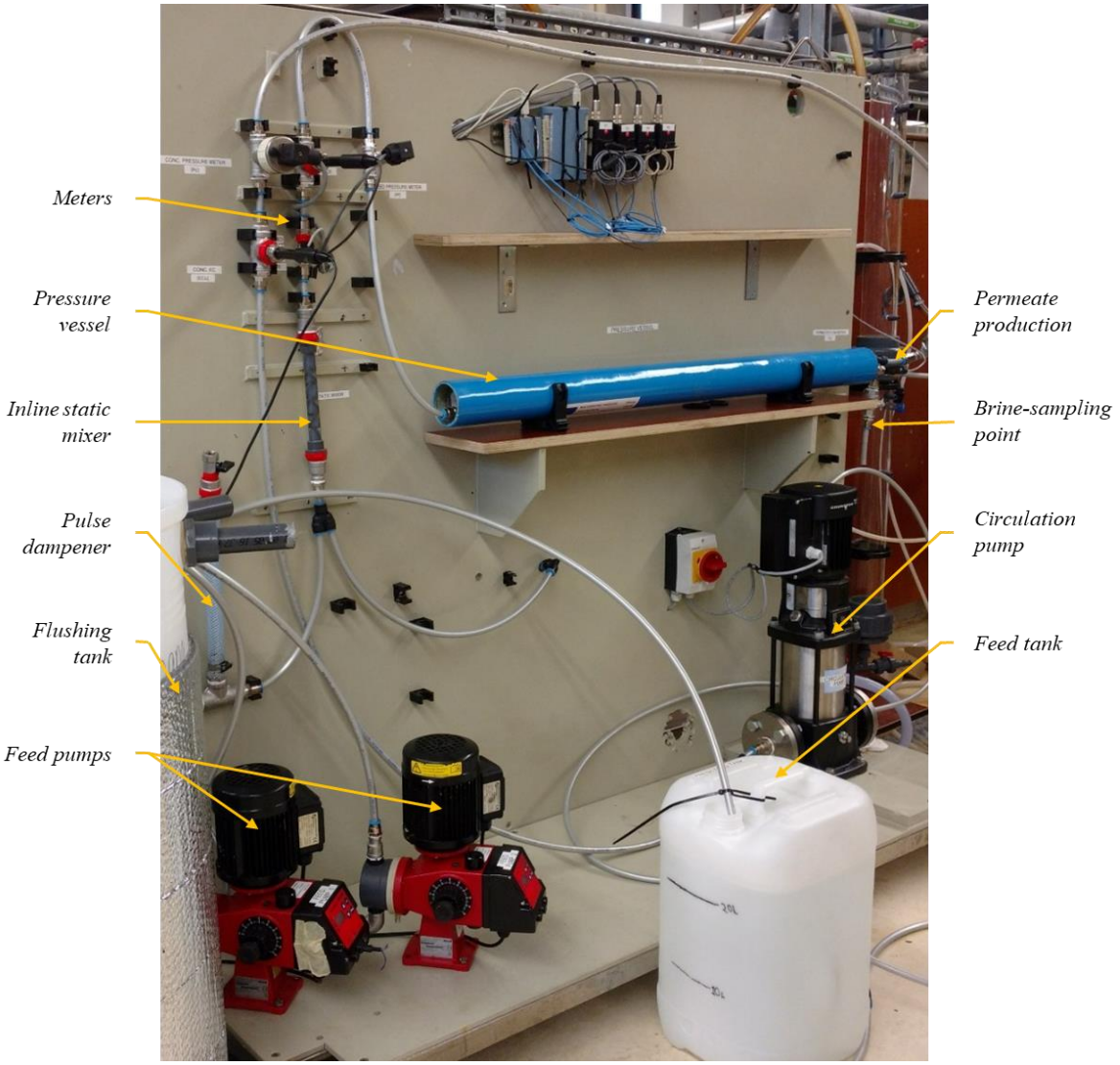

Figure 9. The CCD setup used for the research.

Figure 10 shows the Process and Instrumentation Diagram (P&ID) of the CCD setup. The legend is displayed in Table 2.

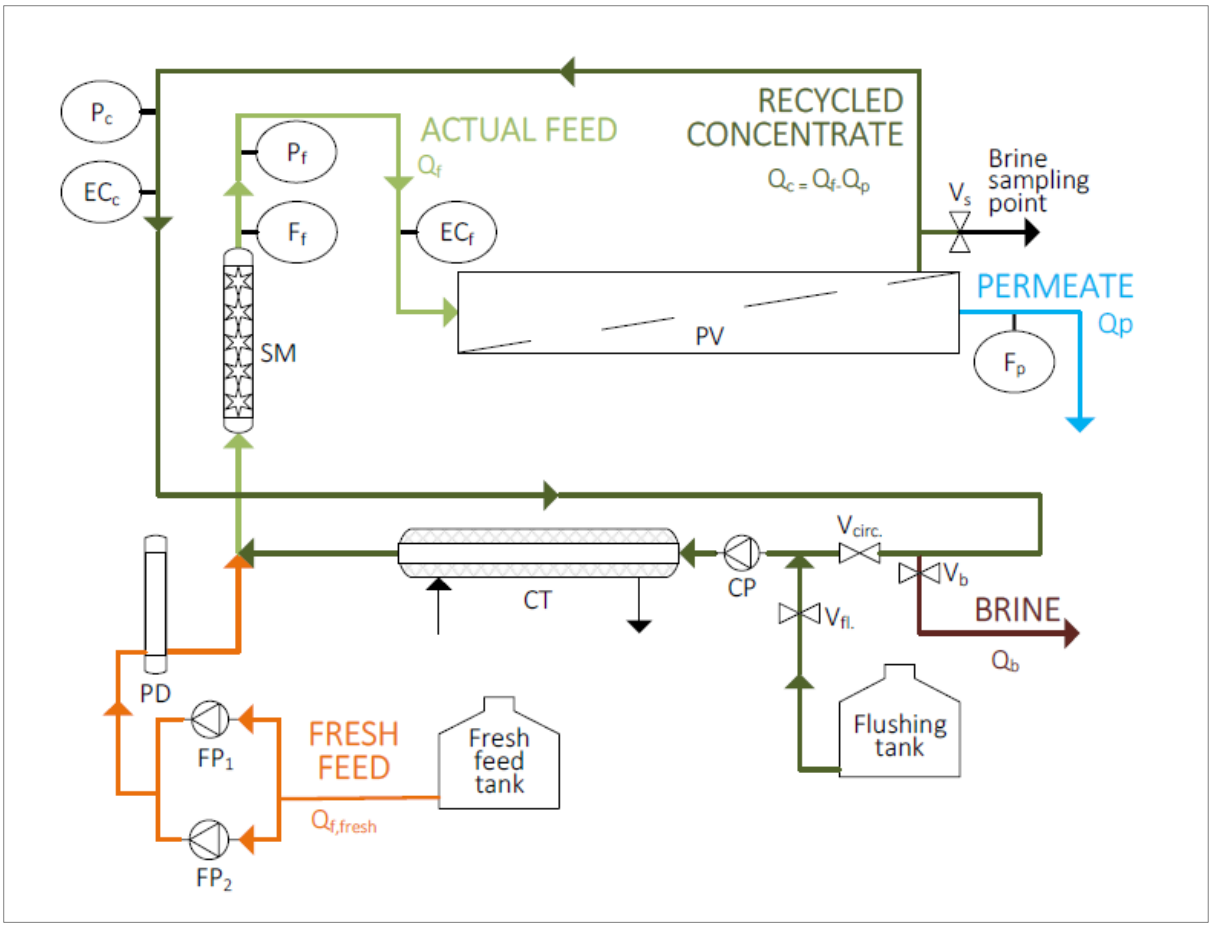

Figure 10. P&ID of the closed-circuit desalination setup.

Table 2. Legend for the P&ID of the CCD setup.

Element	Abbreviation	Description
Components	CT	Cooling tube
	PD	Pulse-dampener
	PV	Pressure vessel
	SM	Static mixer
Meters	EC_f	EC & temperature meter - feed
	EC_c	EC & temperature meter - concentrate
	F_f	Flow meter - feed
	F_p	Flow meter - permeate
	P_c	Pressure meter - concentrate
	P_f	Pressure meter - feed
Pumps	CP	Circulation pump
	FP_1, FP_2	Feed pumps
Valves	V_b	Brine discharge valve
	$V_{circ.}$	Circulation valve
	$V_{fl.}$	Flushing inlet valve
	V_s	Brine-sampling valve

Plastic containers were used as the feed and flushing tanks. Fresh feed was pumped using 2 *Jesco MEMDOS DX 25* feed pumps (FP_1, FP_2), placed in parallel. Each pump could deliver a

maximum flow rate of 25 L/h at up to 10 bars of head. By placing the pumps in parallel, a combined feed flow rate of about 40 L/h was achieved. The concentrate was recirculated with a *Grundfos* centrifugal pump (CP), that could deliver a maximum flow rate of 900 L/h at up to 6 bars of head. The feed flow rate was kept at 30 - 40 L/h and the concentrate flow rate about 400 - 600 L/h. A single RO membrane element (*FILMTEC™ SW30-2540*) was loaded into the pressure vessel.

FESTO Polytetrafluoroethylene (PTFE) tubes of external diameter 12 mm were used for the system along with FESTO pneumatic push-in connectors. The pipes and the junctions of the network could withstand up to 14 bars of pressure. Thus, the pressure maintained in the system was kept below this value.

The flushing inlet ($V_{fl.}$) and brine discharge (V_b) valves were used for the flushing operation. The circulation valve ($V_{circ.}$) was closed during flushing. At the end of a cycle, brine samples were taken at the sampling valve (V_s), placed immediately after the pressure vessel. $V_{circ.}$ and V_s were stainless steel ball valves. $V_{fl.}$ and V_b were stainless steel gate valves.

The flow rate was measured with flowmeters in the mixed feed and permeate streams (*Gems Sensors, USA*). The concentrate flow rate was calculated by subtracting permeate flow from feed flow. The pressure was measured with two meters in the mixed feed (*Gems Sensors, USA*) and concentrate (*Endress+Hauser, Switzerland*). The flow and pressure meters were calibrated using manufacturer-provided specifications. The readings of the flow meters were verified manually with experiments. The EC and temperature readings on the feed and concentrate streams were made using a digital multiparameter meter (*Multi 3420, WTW Germany*). The probes for the meter were connected into the pipe to ensure that the measurements were made directly in the stream, and not in dead zones. The EC of the permeate stream was measured from samples taken every 10 minutes. See Appendix A.1 for specifications of the meters used. Figure 11 shows the installed meters.

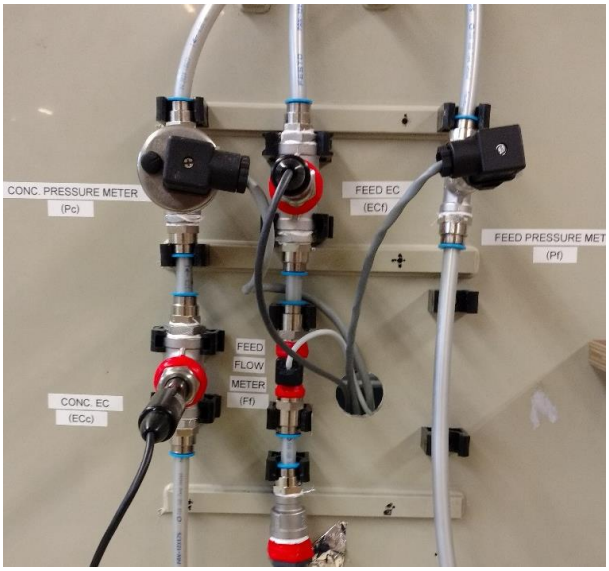

Figure 11. The meters installed on the CCD setup

The feed pumps were dosing pumps. As the pumps delivered feed in pulses, a pulse dampener (PD) was required. A static mixer (*Primix, Netherlands*) was placed before the meters on the feed stream, to ensure adequate mixing of the fresh feed with the recycled concentrate. Thus, the EC measurements taken were representative of the feed. (Refer to Appendix A.2 for the design of the static mixer). An in-line cooling tube (CT) was used to maintain a steady temperature during the experiments because temperature of water in the loop increased with recirculation by the centrifugal pump.

3.2.2. Operation Protocol

The system was flushed with feed water for 10 minutes, before the start of each cycle. The circulation pump (CP) was used for this forward-flushing, to generate enough cross-flow velocity over the membrane. The flow rate during flushing was 400 to 500 L/h. There were some dead-zones in the system that were created during flushing, e.g. between the valves $V_{fl.}$ and V_b. To dilute and remove any trapped brine, recirculation with the feed pumps (FP_1, FP_2) was done during the forward-flush operation. During recirculation, the flushing inlet valve ($V_{fl.}$) and brine discharge valve (V_b) were kept closed and the circulation valve ($V_{circ.}$) open.

After flushing, the filtration cycle was started. The feed pumps were started, followed by the circulation pump. A fresh feed sample was taken from the feed tank. The permeate EC was measured every 10 minutes from collected samples. Once the cycle time was complete, the pumps were stopped, and brine samples were collected from the brine sampling point (V_s). After sampling, flushing was started. The protocol was repeated for the next cycle. Figure 12 summarises the protocol followed for the experiments.

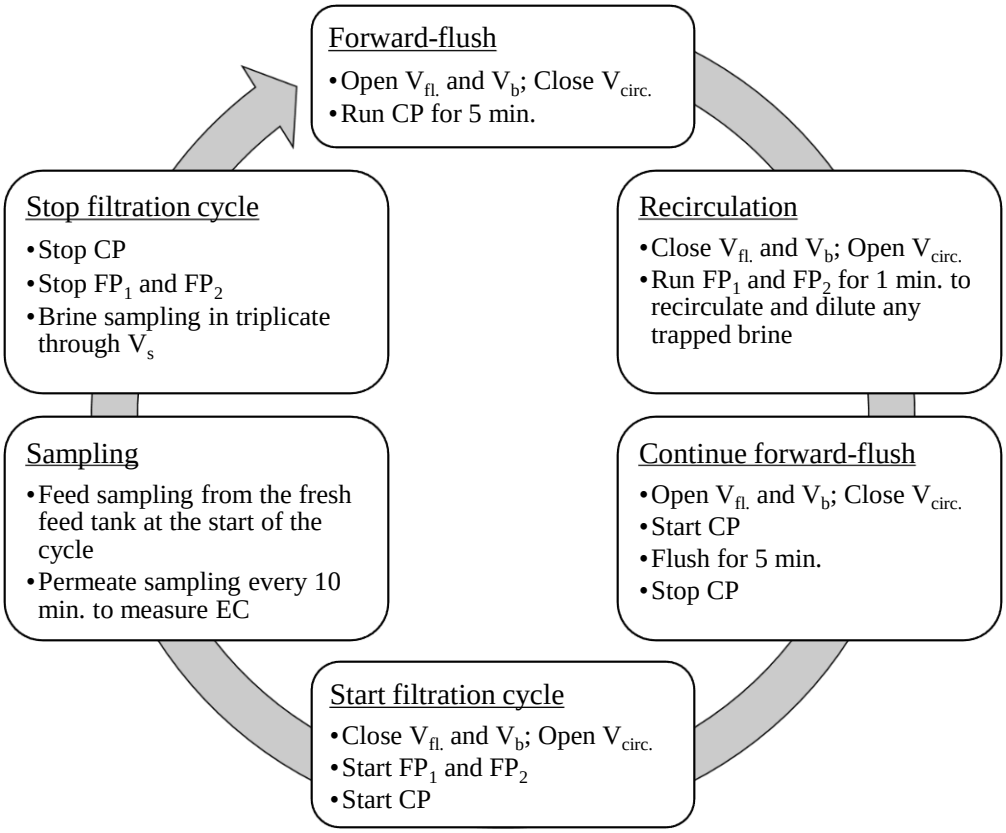

Figure 12. Operation protocol for each cycle.

3.2.3. Experiments

Five series of experiments were performed, as follows:

i. Series A: Initial experiments

Experiments were performed with plain demineralised water, and with feed containing silica with NaCl. The silica concentration was varied: 35 mg/L, 70 mg/L and 80 mg/L as SiO_2. The

concentration of NaCl was kept constant at 10 mg/L. The experiments consisted of a single 1-hour cycle for each feed concentration.

ii. Series B: Experiments with 70 mg/L silica

This series of experiments consisted of 5 cycles of 1 hour each, with feed water consisting of 70 mg/L SiO_2 and 10 mg/L NaCl. The calculation of silica mass was done for this and for the following series of experiments.

iii. Series C: Consecutive experiments with 120 mg/L silica

This series of experiments consisted of 20 cycles of 1 hour each, with 120 mg/L SiO_2 and 10 mg/L NaCl in the feed water. The experiments were conducted with a fresh membrane element.

iv. Series D: Experiments with increased cycle duration with 120 mg/L silica

This series of experiments consisted of 2 cycles of 3 hours each, with 120 mg/L SiO_2 and 10 mg/L NaCl in the feed water. For this series, a fresh element was installed.

v. Calculation of system volume

It is important to calculate the system volume. In CCD, the system volume determines the volume of brine generated at the end of each cycle, and consequently the system recovery. To enable easy calculation of the volume, feed consisting only of $MgSO_4$ was used. The high rejection of $MgSO_4$ would ensure that the concentration of salt in the permeate would be zero. The feed was prepared by dissolving 50 mg/L of $MgSO_4 \cdot H_2O$ in the demineralised water. As the EC is linearly proportional to the concentration of $MgSO_4$, the EC was monitored to make the volume calculations. The calculations are explained in Section 3.5.4.

3.3. The Reverse Osmosis Membrane

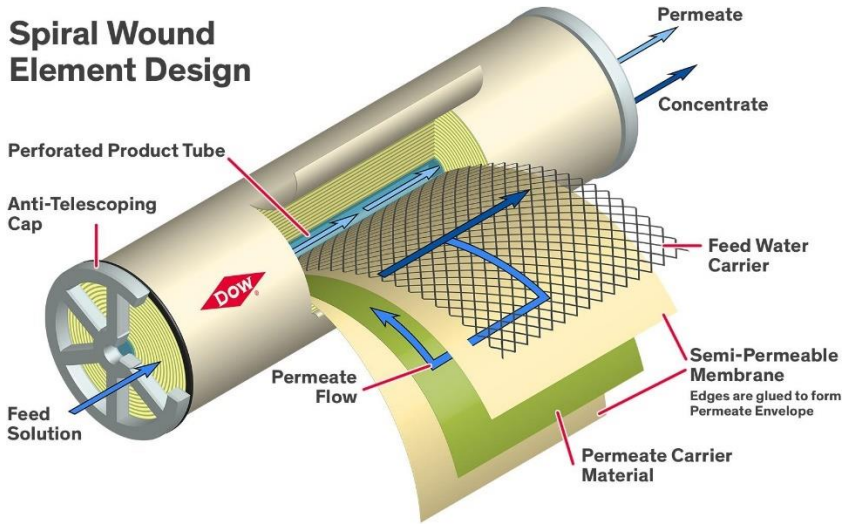

Figure 13. Design of spiral-wound elements [24].

Figure 13 shows the design of spiral-wound elements. A feed channel spacer (feed water carrier) is placed between the semi-permeable membrane sheets to create space between the sheets to allow feed water flow. Similarly, a permeate channel spacer (permeate carrier) is

placed on the permeate side of the membrane. The membrane sheets are glued on three sides and then wrapped around a core tube for permeate flow. The edges of the permeate spacers are sealed to this core tube.

The ends of the element are sealed with an anti-telescoping device. A brine seal in placed in a groove on the anti-telescoping device, at the feed side of the element. The brine seal forces the feed to travel through the element and not around it. The brine seal has a U-shaped cross-section, with the flared end facing the feed inlet.

3.3.1. Element Details

FILMTEC™ SW30-2540 elements were used for all the experiments in this research. These are polyamide thin-film composite spiral-wound membranes. The *FILMTEC™* semi-permeable membranes consist of a thin polyamide barrier layer (0.2 µm), a microporous polysulfone layer (40 µm) and a polyester support layer (120 µm) [25]. Figure 14 shows the dimensions of the element.

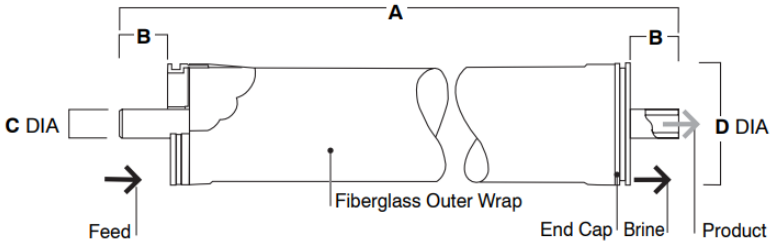

Dimension	Length (mm)
A	1016
B	30.2
C	19
D	61

Figure 14. Dimensions of the SW30-2540 element [26].

3.3.2. Mounting an Element into the Pressure Vessel

The RO spiral-wound element is mounted into a pressure vessel with the end with the brine seal placed on the feed side. The element must be loaded into and removed from the pressure vessel along the direction of feed flow, to prevent slipping or damage of the brine seal. Bearing plates are fitted into the ends on the pressure vessel. The bearing plate has ports to connect to the feed, concentrate and permeate tubes. A locking ring set fits into a groove along the inner surface of the pressure vessel, holding the bearing plate in position. Figure 15 shows the bearing plate on the permeate-concentrate side of the pressure vessel. The three-piece locking ring set is visible.

Figure 15. The bearing plate on the permeate-concentrate side of the pressure vessel.

After loading the element, the pressure vessel was then mounted onto the setup, and the feed, permeate and concentrate tubes connected to their respective ports. Each fresh element was first subjected to an hour of filtration with demineralised water, to flush out any chemicals in the element.

3.4. Analytical methods

3.4.1. Online Measurements

The flow rates of the feed and permeate, and pressures of the feed and concentrate were recorded continuously, with a data acquisition system at a 1-second interval, and then averaged into 5-second intervals. The EC and temperature readings of the feed and concentrate from the digital meter was stored continuously at a 5-second interval using *MultiLab Importer®*, an add-in for MS Excel.

3.4.2. Silica Analysis

The silicomolybdate method was used to analyse soluble SiO_2 (Hach Powder Pillow Method – 8185, *Hach*). This method is based on the reaction of silica and phosphate with molybdate to form silicomolybdic acid complexes (yellow-coloured) under acidic conditions. After a 10-minute reaction time, citric acid is added to destroy any phosphate complexes formed. A spectrophotometer measures the remaining yellow colour, which indicates the SiO_2 concentration. The original sample (without the addition of reagents) is used as a blank to remove interferences by colour and turbidity. [26]

Total silica comprises of reactive (monomer) and non-reactive (polymer) silica. The silicomolybdate method measures only the reactive form of silica present in the solution. Analysis of total silica by ICP-MS failed.

Samples were stored in plastic containers to avoid contamination of silica. When not analysed immediately, samples were stored at 5°C and allowed to warm to room temperature before analysis. As the range of measurement of the test kit was 1 - 100 mg/L of SiO_2; the samples had to be diluted. The samples were diluted with ultrapure water to prevent contamination. The stock and diluted solutions were weighed accurately to 0.01 mg to calculate the dilution factors.

3.4.3. ICP-MS Analysis

Inductively Coupled Plasma Mass Spectrometry (ICP-MS) was used to measure sodium in the samples. The samples were diluted with ultrapure water and then acidified with 1% ultrapure nitric acid.

3.5. Calculations

The data collected from the online meters was used for calculation of the mass transfer coefficient (MTC) and normalised pressure difference (NPD). The EC of the permeate was measured from samples taken every 10 minutes, with a digital multiparameter meter. The measured values were used to create a trendline to generate a series of values at a 5-second interval.

The flow rate of the recycled concentrate was calculated from the flow rates of the actual feed and permeate (Equation 3.1).

$$Q_c = Q_f - Q_p \tag{3.1}$$

Where, Q_f, Q_c are the flow rates of the feed and recycled concentrate, respectively, in *L/h*.

The flux through the membrane is calculated as shown in Equation 3.2.

$$J = \frac{Q_p}{A_{mem}} \tag{3.2}$$

Where,

J is the flux through the membrane in $L/m^2 \cdot h$; and

A_{mem} is the nominal active surface area of the membrane element in m^2. For the *SW30-2540* element, this value is 2.7 m^2.

3.5.1. Calculation of Mass Transfer Coefficient (MTC)

The mass transfer coefficient (MTC) was calculated with Equation 3.3 [27].

$$MTC = \frac{Q_p \cdot TCF_{MTC}}{A_{mem} \cdot NDP} \tag{3.3}$$

Where,

MTC is expressed in $m/s \cdot kPa$;

Q_p is expressed in m^3/s;

A_{mem} is expressed in m^2;

TCF_{MTC} is the temperature correction factor for MTC (*dimensionless*); and

NDP is the normalised driving pressure in *kPa*.

TCF_{MTC} was calculated with Equation 3.4.

$$TCF_{MTC} = e^{U\left(\frac{1}{T_f+273} - \frac{1}{T_{ref}+273}\right)} \tag{3.4}$$

Where,

U is a membrane-dependent constant (*dimensionless*);

T_f is the measured feed temperature (°*C*);

T_{ref} is the standard reference temperature (°*C*).

A U value of 3200 was used; based on experiments by PWN and Kiwa [28]. The reference temperature 25°C is chosen because the feed to the CCD system in practice would be a by-product of water production. Thus, it would not have low temperatures, as compared to freshly-extracted ground water.

The normalised driving pressure (NDP) was calculated with Equation 3.5:

$$NDP = \left(\frac{P_f + P_c}{2} - P_p\right) - \left(\frac{\pi_f + \pi_c}{2} - \pi_p\right) \tag{3.5}$$

Where,

NDP is expressed in *kPa*;

P_f, P_c, P_p are the pressures of the feed, concentrate and permeate, respectively, in *kPa*; and

π_f, π_c, π_p are the osmotic pressures of the feed, concentrate and permeate, respectively, in *kPa*.

The osmotic pressure is calculated with Equation 3.6:

$$\pi_i = x_{EC \to TDS} \cdot x_{TDS \to \pi} \cdot EC_i \cdot TCF_\pi \tag{3.6}$$

$$TCF_\pi = \frac{273 + T_i}{273 + T_{ref}} \tag{3.7}$$

Where,

$x_{EC \to TDS}, x_{TDS \to \pi}$ are factors that convert EC to osmotic pressure;

EC_i is the electrical conductivity in *µS/cm*;

TCF_π is the temperature correction factor for osmotic pressure (*dimensionless*); and

T_i is the temperature in *°C*.

The conversion factors ($x_{EC \to TDS}, x_{TDS \to \pi}$) were calculated based on the dissolved salts and the measured EC [27].

3.5.2. Calculation of Normalised Pressure Difference (NPD)

Monitoring the pressure difference across a membrane is important as it is an indicator for fouling. The normalised pressure difference (NPD) is calculated with Equation 3.8 [27].

$$NPD = \Delta P_a \cdot TCF_{\Delta P} \cdot QCF_{\Delta P} \tag{3.8}$$

$$\Delta P_a = P_f - P_c \tag{3.9}$$

Where,

NPD is expressed in *bars*.

ΔP_a is the actual pressure difference across the pressure vessel, in *bars*;

$TCF_{\Delta P}$ is the temperature correction factor for the normalisation of pressure difference (*dimensionless*);

$QCF_{\Delta P}$ is the correction factor for feed flow through the pressure vessel (*dimensionless*); and

P_f, P_c are the pressures of the feed and concentrate, respectively, in *bars*.

$TCF_{\Delta P}$ is calculated with Equation 3.10.

$$TCF_{\Delta P} = \left(\frac{\eta_{T_{ref}}}{\eta_{T_{act}}}\right)^n \tag{3.10}$$

Where,

n is an experimentally-determined constant (n = 3.4); and

η_T is the viscosity (*cP*) at temperature T (°*C*), calculated with Equations 3.11 and 3.12.

The viscosity values were calculated with Equations 3.11 and 3.12.

$If\ 0°C\ < T < 20°C,$

$$^{10}\log \eta_T = \frac{1301}{998.333 + 8.1855 \cdot (T-20) + 0.00585 \cdot (T-20)^2} - 3.30233 \qquad (3.11)$$

$If\ 20°C\ < T < 100°C,$

$$^{10}\log \frac{\eta_T}{\eta_{20}} = \frac{1.3272 \cdot (20-T) - 0.001053 \cdot (T-20)^2}{T + 105} \qquad (3.12)$$

$QCF_{\Delta P}$ corrects the pressure-value for the actual flow per stage. For this single-element setup, a value of 1 was used.

3.5.3. Silica Mass Balance

If the silica concentration measured in the brine ($X_{SiO_2,brine}$) is lower than the expected concentration ($X_{SiO_2,expected}$), there is silica retention in the system, indicating scaling. The expected final concentration of silica in the brine was determined with Equation 3.13.

$$X_{SiO_2,expected} = X_{SiO_2,initial} \cdot CF \qquad (3.13)$$

Where,

$X_{SiO_2,initial}$ is the initial silica concentration, i.e. the silica concentration in the fresh feed, in *mg/L*; and

$X_{SiO_2,expected}$ is the expected silica concentration in the brine, in *mg/L*;

CF is the concentration factor of the system.

The formula for the calculation of CF was derived from the mass balance of the Na-concentration, as seen in Appendix A.4.

$$CF = \frac{EC_c - EC_p}{EC_f - EC_p} \qquad (3.14)$$

The system recovery (γ_{sys}) is calculated from the CF, as shown in Equation 3.15.

$$\gamma_{sys} = 1 - \frac{1}{CF} \qquad (3.15)$$

3.5.4. Calculation of System Volume (V_{sys})

The system volume was calculated using the CF value (calculated as seen in Appendix A.4), with equation 3.16. (The derivation of the formula is seen in Appendix A.5).

$$V_{sys} = \frac{Q_p \cdot t_{cycle}}{CF - 1} \qquad (3.16)$$

3.6. Membrane Analysis

Microscopy and autopsy of the membranes were performed. After each experiment was complete, the element was flushed with demineralised water to remove any brine retained inside the element. Next, the element was removed from the pressure vessel and stored at 5°C. The anti-telescoping caps at the ends of the element were cut off, as seen in Figure 16. Next, the outer fibre-glass shell was removed, as seen in Figure 17.

Figure 16. Cross-section of the element before removal of the fibre-glass shell.

Figure 17. The element after removal of the anti-telescoping caps and fibre-glass shell.

Figure 18. The spread-out sheets of an element.

Figure 18 shows a spread-out element.

The membrane used for the 70 mg/L experiments as showed particle retention, mainly brownish-red particles, probably iron from corrosion of some metal connections in the system.

There was no visual indication of scaling on the membrane. Figure 19 shows the particles observed on the membranes.

Figure 19. Particle fouling on the membrane used for the 70mg/L experiment.

3.6.1. Microscopy

Coupons of 10 cm × 10 cm were cut from the membranes for visual inspection under the microscope. The coupons were rinsed with demineralised water to remove particles before inspection.

3.6.2. Autopsy

Membrane autopsies were performed on the elements used for the experiments. An autopsy can confirm whether minerals are retained on the membrane. For the autopsy, coupons of 5 cm by 5 cm were prepared. The coupons were rinsed with demineralised water to remove particles before analysis. Coupons from a fresh RO element were used as a blank sample. The sampling points of the coupons are shown in Appendix A.3.

The coupons were analysed by the ASTM D6357 method. The elements were measured by Inductively Coupled Plasma Atomic Emission Spectroscopy (ICP-AES).

Chapter 4

Results & Discussion

4.1. Series A: Initial Experiments

The results of the experiment series A were used to select a suitable concentration of silica in the feed and to select a suitable cycle duration for the experiments. In addition to this, improvements were made on the experiment protocol.

There were several issues with this series of experiments. Initial flushing was done with demineralised water, i.e. at the start of the cycle, the system was filled with demineralised water and not fresh feed. Consequently, the feed was diluted in the beginning of the experiment. For the experiments to follow, flushing was done with feed water. The flushing was done with the feed pumps. This resulted in very low flushing flow rate. For the next experiments, the circulation pump was used.

For this series, the permeate EC was calculated by mass balance from the EC of the feed and concentrate. As the ratio of the feed and concentrate EC values to the permeate was very big, this resulted in inaccurate values of the permeate EC. For the experiments to follow, the EC was measured by sampling the permeate every 10 minutes.

The results of this experiment series are displayed in Appendix B.1.

4.2. Series B: Experiments with 70 mg/L silica

This section discusses the results of the experiments series consisting of 5 cycles of 1-hour each with 70 mg/L silica in the feed.

The MTC values were in the range of 0.38×10^{-8} to 0.43×10^{-8} m/s·kPa. The curves of the first 3 cycles were straight, without any decline. The 4^{th} and 5^{th} cycles started at a slightly higher value but eventually merged with the other curves, 40 minutes into the experiment. Figure 20 shows the MTC graph of the 5 cycles. Clearly, there was no sudden decline in the MTC curve;

and the MTC values of the consecutive cycles were the same or slightly higher than the previous cycles.

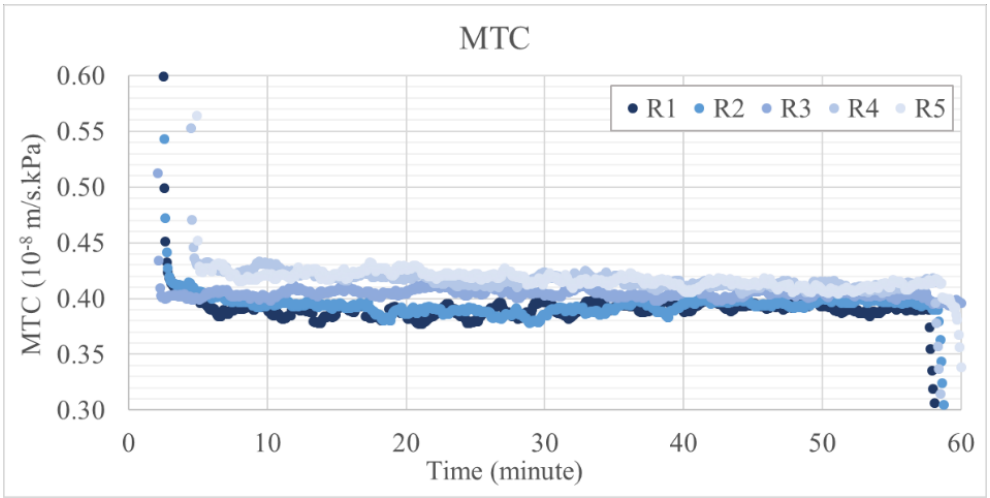

Figure 20. Mass transfer coefficient (MTC) graph for the 5 cycles of the 70 mg/L silica experiment.

Normalised pressure difference: The value remained constant at about 1.2 bar, as seen in the NPD graph (Appendix B.2.1).

Flux and Recovery: The average flux was about 13 to 14 L/m^2·h (Appendix B.2.2). The system recovery was about 82% to 84% at the end of the 1-hour sequence (Appendix B.2.3).

Feed and Concentrate Pressures: Studying the pressure variation in an experiment is important. With increasing osmotic pressure of the feed, more pressure is needed to push the water through the membrane, against the natural osmotic flow. Thus, the feed and concentrate pressure is expected to either remain constant or increase in an experiment. For this experiment series, the pressures decreased by about 0.4 bar for the first 20 minutes of each cycle, before becoming steady for the rest of the experiment (Refer to Appendix B.2.4). The decrease in pressure can be explained using the temperature graph (Appendix B.2.5). The average temperature in loop increased by about 4°C for the first 20 minutes before stabilising. Higher temperatures result in less viscous water, requiring less pressure required. Hence, the pressure required for the first 20 minutes was higher than the rest of the sequence. If there had been fouling or drastic increase in the osmotic pressure, an increase in the pressure would have been observed.

The silica concentration in the final brine was about 430 to 520 mg/L.

4.3. Series C: Consecutive experiments with 120 mg/L silica

This section discusses the results of the experiments series consisting of 20 cycles of 1-hour each with 120 mg/L silica in the feed.

Figure 21 to Figure 24 show the MTC and NPD graphs for this experiment. All the cycles showed the same pattern of decline in the MTC curve along the sequence. However, this decline was not permanent as the original initial MTC value was recovered at the start of the following cycle.

For the first 5 cycles, the MTC values were in the range of 0.44 to 0.48 × 10^{-8} m/s·kPa. There was a slight decline in the MTC curve along the sequence, of the first 2 cycles. The 3rd, 4th and 5th cycles had almost constant MTC values. The MTC curves of all the cycles merged towards to last 10 minutes of the cycle.

For the 6th to 15th cycles, the MTC was in the range of 0.46 to 0.5 × 10^{-8} m/s·kPa and declined to 0.45 × 10^{-8} at the end of the cycle. There is very little variation between the MTC curves of the cycles. In the last 5 cycles, the value was between 0.47 to 0.50 × 10^{-8} m/s·kPa and decline slightly by 0.2 × 10^{-8} m/s·kPa.

Normalised pressure difference: The NPD value dropped from 0.9 bar in the first 5 cycles to 0.8 bar in the next 5 cycles. For the last 10 cycles, it was about 1.08 bar.

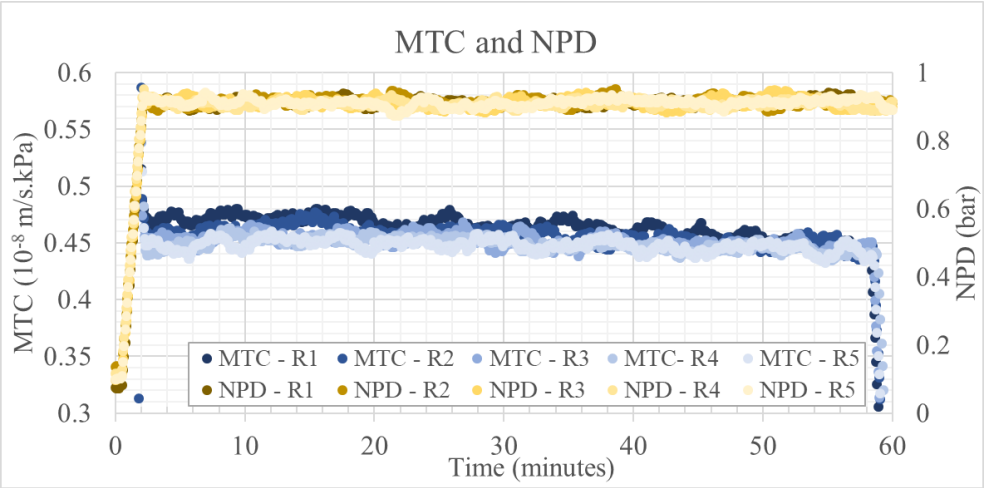

Figure 21. MTC and NPD for R1 to R5 of the 120 mg/L silica experiment.

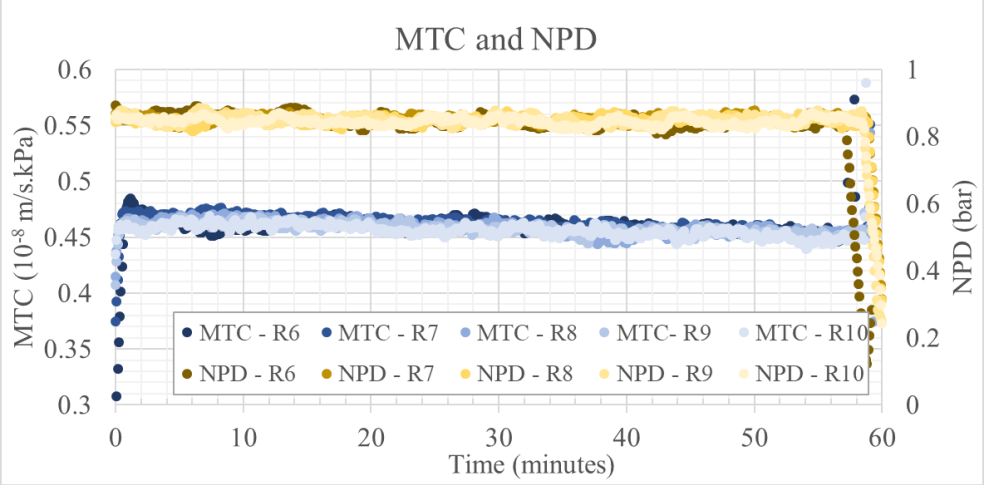

Figure 22. MTC and NPD for R6 to R10 of the 120 mg/L silica experiment.

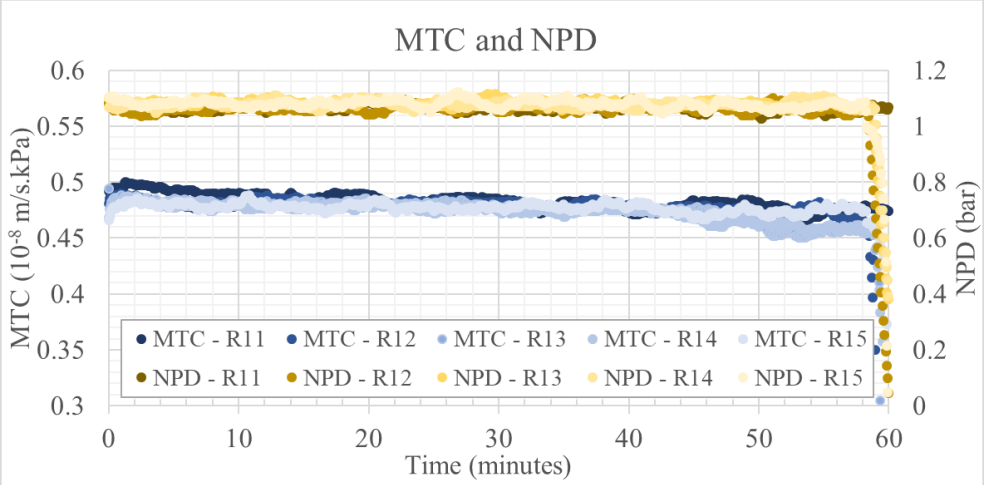

Figure 23. MTC and NPD for R11 to R15 of the 120 mg/L silica experiment.

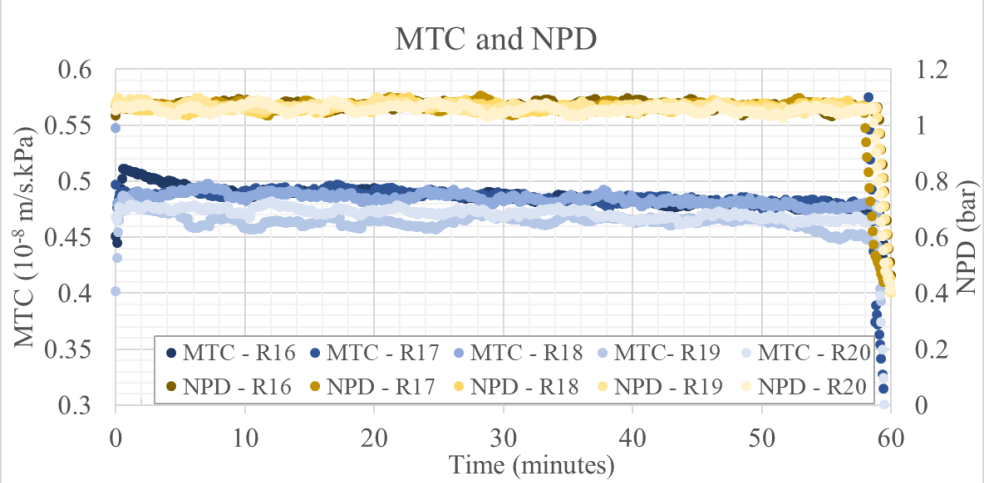

Figure 24. MTC and NPD for R16 to R20 of the 120 mg/L silica experiment.

Flux and Recovery: The average flux in all the experiments was about 13 to 14 L/m^2·h. The flux of the 15th cycle was lower than the other cycles by about 0.4 L/m^2·h. This was a result of lower permeate flow rate due a setting on the feed pumps. The system recovery for the cycles ranged from 78% to 86%. The 15th cycle had a lower recovery as a result of the lower permeate flow rate. (Refer to Appendix B.3.1 for the flux and recovery graphs.)

Feed and Concentrate Pressures: The pressures show a similar pattern of decrease by 0.4 bar or less for the first 10 minutes of each cycle before becoming steady, and then increasing slightly towards the end of the experiment. (Refer to Appendix B.3.2 for the graphs.)

The silica concentration in the final brine was about 550 to 870 mg/L.

4.4. Series D: Experiments with increased cycle duration with 120 mg/L silica

Figure 25 shows the MTC and NPD graph for the 3-hour cycles with 120 mg/L SiO_2. The initial MTC value for both cycles was about 0.5×10^{-8} m/s·kPa. The MTC declines gradually through the experiment but recovers its original value at the start of the 2nd cycle. The MTC curve of

the second cycle has a less steep decline due to a leak in the system, which led to the loss of some concentrate, resulting in a less concentrated stream, and consequently, higher MTC values. The effect of this leak is seen in the graphs of the online EC measurements (Appendix B.4.1).

Normalised pressure difference: The NPD values were 1.05 bar for the 1st cycle and increased to 1.08 bar in the 2nd cycle.

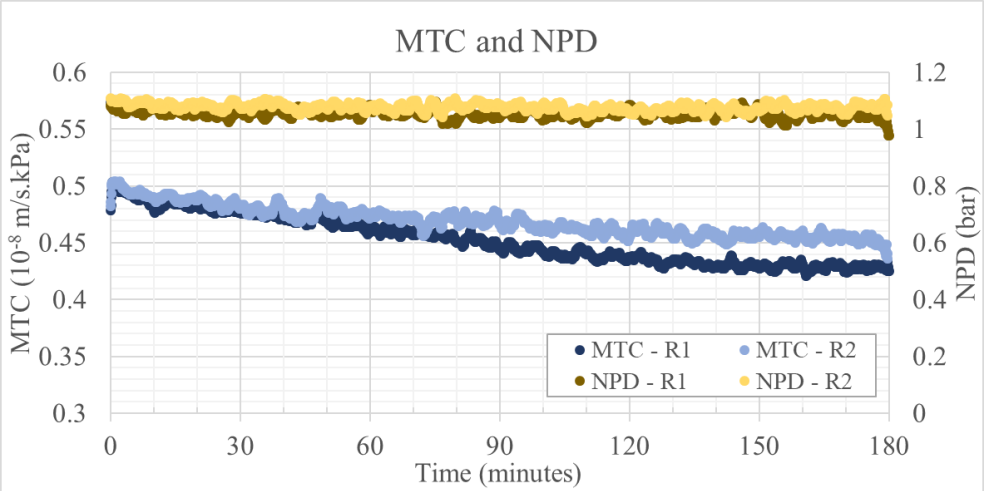

Figure 25. MTC and NPD for the 120 mg/L silica experiment with 3-hour cycle duration.

Flux and Recovery: The flux was about 13 to 14 L/m^2·h. The recoveries of the 1st and 2nd cycles were 93% and 90%, respectively (Refer to Appendix B.4.2).

Feed and Concentrate Pressures: For the first hour, the feed and concentrate pressures followed the same curve as the other 1-hour cycles. However, the pressures gradually increased by 2 bar and 1.3 bar for the 1st and 2nd cycles, respectively. This pressure increase corresponds to the increasing pressure required to produce permeate (Refer to Appendix B.4.3).

The silica concentration in the final brine was 1800 and 1320 mg/L in the 1st and 2nd cycles, respectively.

4.5. Discussion on NPD and MTC

The average flux for all the experiments was 13 to 14 L/m^2·h. The normalised pressure difference (NPD) is an indication of biological or particle fouling. With more clogging of the feed spacer, the resistance increases, resulting in a pressure drop across the membrane. The 70 mg/L experiment (Series B) had the highest NPD, 1.2 bar. A fresh element had not been used for this series of experiments. The same element was used for the initial experiments and the numerous system-check tests, resulting in particle fouling. This could explain the high NPD observed in this experiment, compared to other experiments. This is corroborated by the particle fouling observed on the membrane used for this experiment (as seen earlier in Figure 19).

The mass transfer coefficient (MTC) curves showed a gradual decline but always recovered at the start of the following cycle. That is, the decline in MTC was not permanent, even in the 3-hour cycles with 120 mg/L of silica in the feed. The decline was probably due to the increasing osmotic pressure in the recirculation loop. Moreover, increasing the feed silica concentration

and increasing the cycle duration did not have an effect on the average MTC measured. Thus, there was no indication of loss in permeability as a result of high silica concentrations in the brine, leading to the conclusion that there was no scaling in the system.

4.6. Silica Mass Balance Results

The silica mass balance was calculated from the expected and measured concentrations of silica. The results are displayed in Table 3. The colour codes are explained as follows:

Excess mass
No loss of mass
Loss of mass

Values between -10% and 10% were assumed to mean there was no loss of silica between the measured and expected values. Values lower than -10% meant there's excess mass measured in the system. Values higher than 10% meant there's a loss in mass, i.e. depletion of reactive silica from the concentrate, possibly forming precipitates. Only 2 cycles showed a loss in mass.

The flow rate of flushing for the 70 mg/L experiment and the first 5 cycles of the 120mg/L (1-hour cycles) experiment was not high enough (as flushing was done with the feed pumps). Inadequate flushing between cycles might have caused retention of some brine in the system, causing higher salinity in the system at the start of the next cycle. The final measured concentration of silica would have been higher as a result. This explains the excess mass seen in 3 out of 5 cycles of the 70 mg/L experiment. However, there was no effect observed on the first 5 cycles of the 120 mg/L (1 hour) experiment. In the 120 mg/L experiment (1-hour cycle), out of 20 cycles, 18 cycles showed no loss of mass. In the 120 mg/L experiment (3-hour cycle), the second cycle showed excess mass. However, the results of this cycle are unreliable as a result of a severe leak in the pump flange.

Table 3. Calculation of the silica mass balance for the experiments.

Experiment	Cycle	CF	SiO_2 concentration in the brine	SiO_2 mass balance $\frac{Expected - Measured}{Expected\ concentration} \times 100$
-	-	-	*mg/L*	*%*
70 mg/L SiO_2 – 1h	1	5.9	486	17
	2	6.2	434	-11
	3	6.4	444	-6
	4	5.9	493	-20
	5	5.9	521	-26
120 mg/L SiO_2 – 1h	1	6.7	708	12
	2	7.0	794	5
	3	7.0	836	0
	4	7.0	873	-4
	5	7.0	825	1
	6	6.0	656	8
	7	5.4	674	-5
	8	6.6	745	6
	9	5.5	716	-9
	10	5.1	652	-7
	11	6.3	733	4
	12	5.9	781	-11
	13	6.0	753	-5
	14	6.6	857	-9
	15	4.6	549	1
	16	6.6	763	9
	17	5.1	670	-4
	18	6.0	732	3
	19	6.9	871	1
	20	6.3	799	1
120 mg/L SiO_2 – 3h	1	14.2	1800	-6
	2	9.8	1324	-12

To conclude, there was no loss of silica in the mass balance calculations, signifying the absence of scaling. The reactive silica concentration in the brine was as high as 1800 mg/L in the 3-hour cycle, attaining a recovery of 93%.

Figure 26 shows the monomeric silica concentration measured in the brine at the end of each cycle. These concentrations were attained without noticeable scaling.

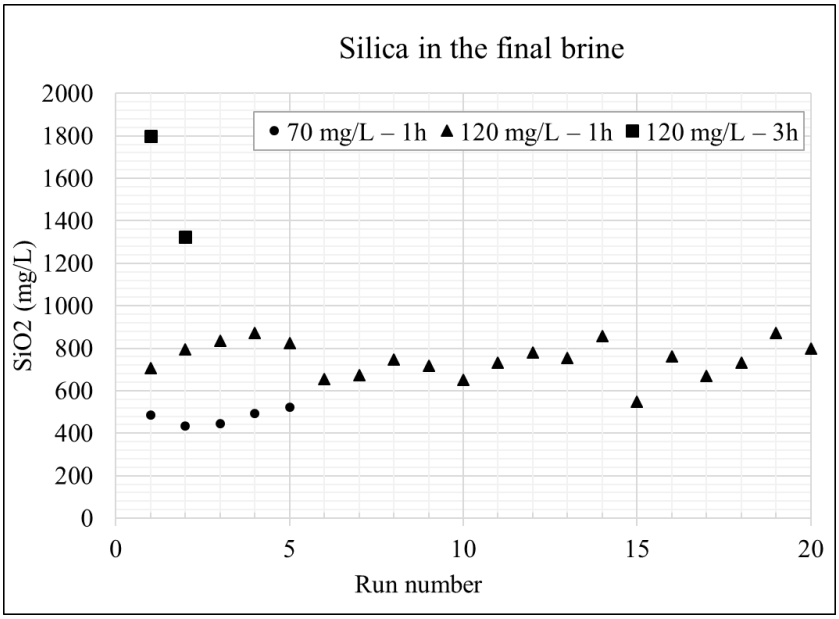

Figure 26. Silica concentration in the brine at the end of the experiment.

4.7. Calculation of System Volume

In CCD, the system volume determines the volume of brine generated at the end of each cycle, and consequently the system recovery. The standard system volume was calculated by conducting a 1-hour experiment with feed containing only $MgSO_4$ in the feed. The rejection of $MgSO_4$ observed was 100%. The concentration factor of the system was 5.85 for a 1-hour cycle duration. The calculated system volume was 7.67 L.

The standard system volume was compared to the other cycles to determine the influence of the pump flange leakage on the quality of the experiments. Thus, the calculation of the system volume was also a verification for the quality of each experiment.

The standard value was compared to the volume calculated for other experiments using the concentration factor (CF) at the end of each cycle. For the 3-hour cycles, the values of CF at the end of an hour was used for the calculation of the system volume, for comparability to the system volume of the $MgSO_4$ experiment. The results are displayed in Table 4. The colour codes are explained as follows:

Lower volume
System volumes match
Higher volume

Values in the range of -10% to 10% were assumed to be equal to the standard system volume. Values lower than -10% meant that the calculated volume was lower than the standard. Values higher than 10% meant that the calculated volume was higher than the standard. Higher system volumes were the influence of the pump leakage. Lower system volumes could be caused by inadequate flushing between consecutive cycles.

As mentioned earlier, inadequate flushing results in a higher final concentration of the brine, resulting in a higher CF. Referring to the formula for the calculation of system volume, a higher

CF results in a lower system volume. For the experiments which had insufficient flushing (70 mg/L experiment and the first 5 cycles of the 120mg/L (1-hour cycles) experiment), 7 out of 10 cycles had a lower system volume.

Out of the remaining experiments which had sufficient flushing, 15 out of 17 experiments matched system volumes to the standard. Four cycles showed higher volumes, as a result of the leak.

Table 4. Calculation of the system volume for the experiments.

Experiment	**Cycle**	**CF (at 1 hr)**	**Average Q_p**	**Sequence time**	**Calculated system volume**	**Difference with $MgSO_4$ experiment**
-	-	-	*L/h*	*min*	*L*	*%*
$MgSO_4$ - 1h	-	5.9	37	60	7.7	Standard
70 mg/L - 1h	1	5.9	35	60	7.0	-9
	2	6.2	34	62	6.8	-12
	3	6.4	36	60	6.7	-13
	4	5.9	36	60	7.4	-3
	5	5.9	37	60	7.5	-2
120 mg/L - 1h	1	6.7	39	60	6.7	-12
	2	7.0	38	60	6.4	-17
	3	7.0	39	60	6.5	-16
	4	7.0	39	60	6.5	-15
	5	7.0	39	60	6.5	-15
	6	6.0	37	59	7.3	-5
	7	5.3	36	61	8.4	10
	8	6.6	38	61	6.9	-10
	9	5.5	37	60	8.2	7
	10	5.1	36	61	8.8	15
	11	6.3	37	62	7.2	-6
	12	5.9	37	60	7.7	0
	13	6.0	37	61	7.5	-2
	14	6.6	38	61	7.0	-9
	15	4.6	35	60	9.7	26
	16	6.6	38	61	6.8	-11
	17	5.1	36	59	8.7	14
	18	6.0	38	61	7.6	0
	19	6.9	38	60	6.5	-16
	20	6.3	38	60	7.2	-6
120 mg/L - 3h	1	5.7	36	60	7.7	1
	2	5.0	36	60	8.9	16

4.8. Membrane Analysis Results

4.8.1. Microscopy Results

Figure 27 shows the images of the blank membrane analysed under the microscope, at 20- and 120-times magnification.

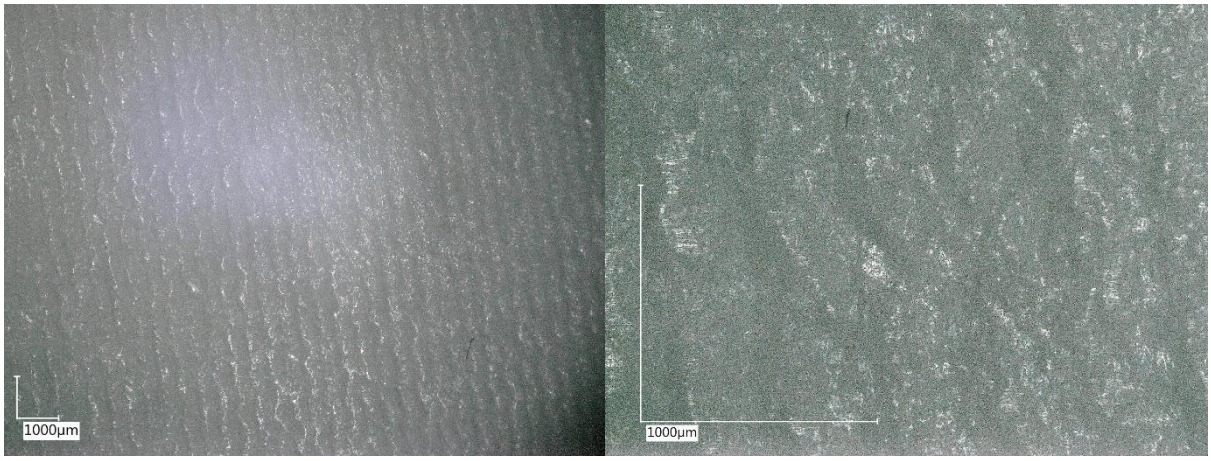

Figure 27. Microscopy of the blank membrane; Magnified 20 times (left) and 120 times (right).

Figure 28 and Figure 29 depict images of the membrane used for the 20 consecutive cycles with 120 mg/L silica in the feed (Experiment series C). There is particle fouling on the membrane, along the feed spacer, resulting in the pattern of the spacer on the membrane, as seen in Figure 28.

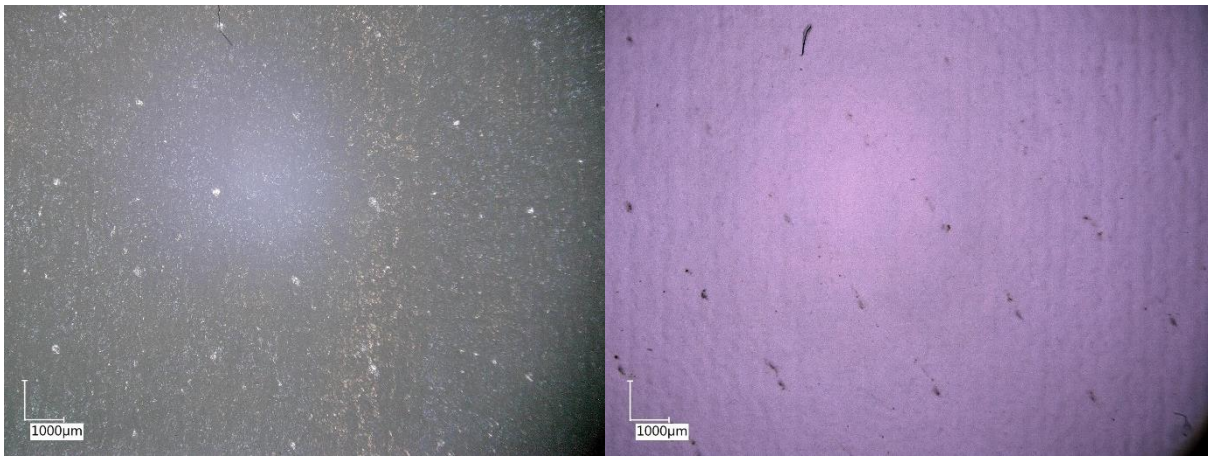

Figure 28. Microscopy of the membrane used for experiment series C; magnified 20 times, under different light settings.

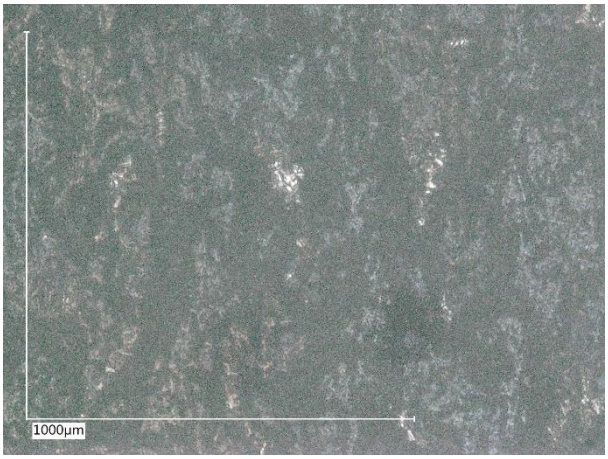

Figure 29. Microscopy of the membrane used for experiment series D; magnified 200 times.

Figure 30 depicts images of the membrane used for the 3-hour cycles with 120 mg/L silica in the feed (Experiment series D).

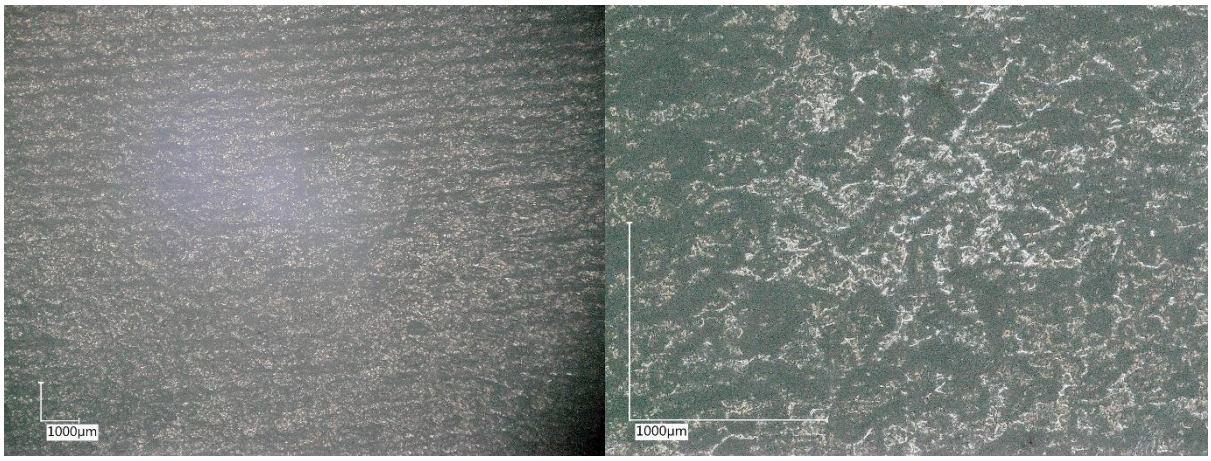

Figure 30. Microscopy of the membrane used for experiment series D; Magnified 20 (left) and 100 times (right).

Comparing the images of the membranes used for experiment series C and D to the blank, there was no visible evidence of scaling observed.

4.8.2. Autopsy Results

Table 5 is a compilation of the membrane autopsy results. The exact point of sampling for each coupon is illustrated in Appendix A.3. The values of Al, Ca, Cu, Fe, Mg and Mn were below detection levels (10 µg/cm^2 for Al; 5 µg/cm^2 for Ca, Cu, Fe, Mg and Mn).

Table 5. Membrane autopsy results.

Membrane	Sample	Sampling side	Si µg/cm²	K µg/cm²	Na µg/cm²	Ti µg/cm²
Blank	B1	Feed	25	45	850	1370
	B2	Concentrate	30	40	950	1300
Series A, B	M1†	Feed	-	-	-	-
	M2†	Concentrate	(32)	-	-	-
Series C	M3†	Feed	(40)	-	-	-
	M4†	Concentrate	(80)	-	-	-
	M9	Middle	56	45	235	1350
Series D	M5	Concentrate	58	58	270	1350
	M6	Feed	58	66	260	1535
	M7	Concentrate	66	48	275	1395
	M8	Feed	48	56	235	1390

The silicon values in 120 mg/L experiments (Series C and D) are twice to thrice the values on the blank membranes. The blank samples have a relatively high sodium concentration compared to the other samples. This could be attributed to the preservative storage solution of new elements. *FILMTEC*™ membranes are preserved in 1% sodium metabisulfite, preventing biological growth during storage and transport [29]. The titanium and potassium concentrations appear similar to the blank samples.

The membrane autopsy results show that the membranes of the 120 mg/L experiments had higher silicon content per sample area compared to the blank membrane. This could be a sign of scaling, but it is difficult to prove that in a scientific way. If there was scaling, the amount of deposition must have been very little, as there was no loss in the mass balance calculations. This was supported by the MTC curves that showed no permanent decline with consecutive cycles. Furthermore, there was no visual evidence of scaling observed with the microscope, because if there was scaling on the membrane, it is at the initiation stages and only specific parts of the membrane were observed, not the whole.

4.9. Discussion on State of Silica in the System

The brine produced in these experiments were alkaline (pH > 10) with high concentrations of sodium and silica (monomeric). The concentration of silica in the brine was about 15 times the saturation level (118 mg/L) [8], without any scaling. This could be explained by the formation of neutral complexes ($Si_7O_{18}H_4Na_4$) that behave like colloids [31]. These colloids can aggregate up to sizes of 3 nm. When the concentrated solution is diluted, the aggregates decrease in size, eventually disappearing. The brine samples were diluted before the analysis of silica with the silicomolybdate method. Hence, the complexes formed in the brine would have dissociated back into monomeric silica.

† *The analysis of the samples M2, M3 and M4 were done assuming M1 was a blank. Although the exact values might not be correct, they can still be compared among each other.*

At pH > 9, the rate of polymerisation of silica monomers slows down and there is an increase in the solubility of silica [7] [8]. In the current study, silica concentrations of 1800 mg/L were achieved in 3-hour cycles, without seeing significant depletion of monomeric silica. As the pH in the prepared feed was about 10, rate of polymerisation would have been slow. There was no depletion of monomer silica from the brine, as shown by the measurements of monomer silica by the silicomolybdate method. The high pH and the absence of other components such as calcium and magnesium could have delayed polymerisation in such supersaturated conditions. The absence of components such as non-silica colloids, pre-existing scale or corrosion products could have prevented heterogenous scaling of silica. Darton's review of membrane autopsies highlighted the significance of polyvalent cations like iron (Fe^{3+}) and aluminium (Al^{3+}) in silica scaling. Out of 100 membrane autopsies, only a single membrane with silica fouling had neither iron nor aluminium in the deposits [31]. This could mean that there is a risk of scaling in the system, at similar super-saturations of silica, in the presence of these components.

Chapter 5

Conclusion

This research study evaluated the effectiveness of closed-circuit desalination (CCD) in delaying, reducing, or even preventing silica scaling on membranes when dealing with feed containing significant levels of silica. A CCD setup with relevant meters was designed and built. Silica scaling was monitored by MTC and silica mass balance calculations, and by destructive analysis of the membrane. The silica concentration in the feed was increased as high as 120 mg/L as SiO_2; up to 20 consecutive experiments were performed; and the cycle duration was increased from 1 to 3 hours.

The MTC graphs showed a gradual decrease that recovered with flushing at the end of the cycle. There was no permanent decrease in MTC, even at the end of the 3-hour cycle experiments with 120 mg/L silica in the feed.

Scaling would have resulted in the depletion of reactive silica from the brine, which would have created a difference in the mass balance calculations. According to the silica mass balance calculations, there was no significant loss of silica in the brine.

The results of the membrane autopsy showed that the membranes from the 3-hour cycles had higher silicon on the membrane compared to the blank. It is not clear if the higher silicon concentration was a result of scaling or was simply brine residue left on the membrane coupons. As there was no loss in the mass balance calculations, even if there was scaling, it must have been too minimal to see a significant loss in the mass balance calculations. There was no depletion of reactive silica from the brine, despite high supersaturations (about 15 times the saturation level).

Thus, the designed CCD system was resistant to silica scaling in these conditions, of high pH and in the absence of other components such as iron, aluminium, calcium and magnesium. High levels of silica supersaturation in the brine were achieved without the use of anti-scalants. Recoveries over 90% were reached with up to 1800 mg/L silica in the brine, without noticeable scaling. Hence, this validates the ability of this technology to treat RO brine to reclaim as much water from the brine, producing an even more concentrated brine stream, from which extraction

of minerals would be possible, despite high concentrations of silica in the feed. The extremely high recoveries attained by the system would result in small volumes of very concentrated brine, making the extraction of minerals more cost-effective, because lesser volumes at higher concentration must be treated to obtain the same amount of minerals. Cost-effectiveness is crucial if the technologies of mineral extraction are energy-intensive.

The results of this study proved that, despite high concentrations of silica in the feed, CCD can improve the total efficiency of RO systems (with regard to the water wastage) by recovering water from the brine produced by RO installations. This is especially important in the present scenario of growing pressure on natural water sources. The system successfully reached recoveries higher than 90% without the use of anti-scalants.

Chapter 6

Recommendations

The CCD system has been considerably resistant to scaling despite high concentrations. However, there are several issues that need to be studied further before application in practice.

A thorough study of the chemistry of silica in the system is required. This could help understand the effect of other components, and the optimal water quality parameters to maintain, such as the pH and temperature of the system. The pH in the system needs to be monitored, to understand the chemical interactions that take place in the supersaturated brine solution. In this research, only monomeric silica was measured. Measuring total silica (monomeric and polymeric silica) would be required in the event of formation of polymeric silica.

In the 120 mg/L experiments, the ratio of concentrations of Na:SiO_2 in the fresh feed was 1:30.5. A change in this ratio could affect the silica chemistry in the concentrate. In the brine from the *EVIDES* RO plant (ZERO BRINE project), the ratio of Na:SiO_2 is 1:0.03. George reported that high concentrations of NaCl (greater than 15 g/L as NaCl) reduced the induction time and rate of polymerisation, with an initial silica concentration of 400 mg/L [20]. The effect of sodium concentration on the silica chemistry should be investigated.

The membrane autopsy done in this research did not provide absolute indications of scaling. There were too few samples to compare and make a strong conclusion. A more detailed membrane analysis with more samples from each element could provide more conclusive results regarding the deposition of minerals on the membrane.

The pH of the prepared fresh feed was very high (≈ 10) and consisted of only sodium and silica (SiO_2). The presence of calcium and magnesium in solutions at such high pH, with increased solubility of silica increases the potential for scaling. The presence of polyvalent metal ions such as iron or aluminium can cause heterogenous precipitation of monomeric silica. Thus, in the presence of such elements, silica scaling could occur much faster. Experiments should be performed to assess if CCD can prevent scaling in system despite the presence of these components.

In the present study, experiment series C consisted of 20 consecutive cycles of 1 hour each, adding up to 20 hours of cycle-time. There was no scaling observed, as per MTC and mass balance calculations. The results of this research validated the short-term performance of CCD with respect to silica scaling. Experiments in a pilot plant could shed light on the long-term performance of CCD.

Finally, experiments need to be performed using feed water based on the actual RO brine. The complex nature of the brine composition would probably result in different scaling dynamics.

References

[1] R. L. Stover, "High recovery, low fouling, and low energy reverse osmosis," *Desalination and Water Treatment,* pp. 1-6, 2016.

[2] A. Haidari, "One Step Membrane Filtration: A fundamental study," 2017.

[3] J. Kucera, Reverse Osmosis: Industrial Processes and Applications, 2nd Edition, 2 ed., Hoboken, New Jersey: John Wiley and Sons, 2015.

[4] T. Oki and S. Kanae, "Global Hydrological Cycles and World Water Resources," *Science,* vol. 313, no. 5790, pp. 1068-1072, 2006.

[5] ZERO BRINE, "ZERO BRINE," December 2018. [Online]. Available: https://zerobrine.eu/about-us/.

[6] C. van de Lisdonk, B. Rietman, S. Heijman, G. Sterk and J. Schippers, "Prediction of supersaturation and monitoring of scaling in reverse osmosis and nanofiltration membrane systems," *Desalination,* pp. 259-270, 2001.

[7] J. Gill, "Inhibition of silica-silicate deposit in industrial waters," *Colloids and Surfaces A: Physicochemical and Engineering Aspects,* vol. 74, no. 1, pp. 101-106, 1993.

[8] I. Bremere, M. Kennedy, S. Mhyio, A. Jaljuli, G.-J. Witkamp and J. Schippers, "Prevention of silica scale in membrane systems: removal of monomer and polymer silica," *Desalination,* vol. 132, no. 1-3, pp. 89-100, 2000.

[9] R. L. Stover, "Industrial and brackish water treatment with closed circuit reverse osmosis," *Desalination and water treatment,* vol. 51, pp. 1124-1130, 2013.

[10] A. Efraty, R. N. Barak and Z. Gal, "Closed circuit desalination — A new low energy high recovery technology without energy recovery," *Desalination and Water Treatment,* pp. 95-101, 2011.

[11] D. M. Warsinger, E. W. Tow, L. A. Maswadeh, G. Connors, J. Swaminathan and J. H. Lienhard V, "Inorganic fouling mitigation by salinity cycling in batch reverse osmosis," *Water Research,* vol. 137, pp. 384-394, 2018.

[12] A. Efraty, "CCD series no-16: opened vs. closed circuit SWRO batch desalination for volume reduction of Silica containing effluents under super-saturation conditions," *Desalination and Water Treatment,* pp. 9569-9584, 2016.

[13] A. J. Tarquin, M. P. Fahy and J. E. Balliew, "Concentrate Volume Reduction Research In El Paso, Texas," in *World Environmental and Water Resources Congress 2010: Challenges of Change*, Providence, 2010.

[14] J. C. van Dijk, J. Q. J. C. Verberk, S. G. J. Heijman, L. C. Rietveld, D. de Ridder, A. Grefte and P. Andeweg, Drinking Water Treatment, Delft: Delft University of Technology, 2009.

[15] L. F. Greenlee, D. F. Lawler, B. D. Freeman, B. Marrot and P. Moulin, "Reverse osmosis desalination: Water sources, technology, and today's challenges," *Water Research,* vol. 43, pp. 2317-2348, 2009.

[16] S. Lin and M. Elimelech, "Kinetics and energetics trade-off in reverse osmosis desalination with different configurations," *Desalination,* vol. 401, pp. 42-52, 2017.

[17] H. E. Bergna and W. O. Roberts, Colloidal Silica: Fundamentals and Applications, Boca Raton: CRC Press, 2005.

[18] S. D. Freeman and R. J. Majerle, "Silica fouling revisited," *Desalination,* vol. 103, no. 1-2, pp. 113-115, 1995.

[19] D. E. George, "Prediction of Silica Scale Formation in RO Systems," *Desalination,* vol. 47, no. 1-3, pp. 161-169, 1983.

[20] V. Polyakov and S. Polyakov, "On the calculation of reverse osmosis plants with spiral-wound membrane elements," *Desalination,* no. 104, pp. 215-226, 1996.

[21] S. Heijman, H. Folmer, F. Donker, B. Rietman and J. Schippers, "Application of ScaleGuard® at reverse osmosis and nanofiltration installations," *Water Science and Technology: Water Supply,* pp. 133-138, 2003.

[22] Merck, "338443 - Sodium silicate solution," 2018. [Online]. Available: https://www.sigmaaldrich.com/catalog/product/sigald/338443?lang=en&region=NL. [Accessed May 2018].

[23] D. C. Appelo, "SPECIFIC CONDUCTANCE: how to calculate, to use, and the pitfalls," [Online]. Available: https://hydrochemistry.eu/exmpls/sc.html. [Accessed December 2018].

[24] Evoqua Water Technologies, "What is reverse osmosis?," 2018. [Online]. Available: http://www.evoqua.com/en/brands/IPS/Pages/what-is-reverse-osmosis.aspx. [Accessed 8 December 2018].

[25] Dow, "FILMTEC™ Membranes - Basics of Ro and NF: Membrane Description," Dow.

[26] Dow, "FILMTEC™ Seawater Reverse Osmosis < 4" Elements," 2018. [Online]. Available: http://www.dupont.com/products/FILMTECSW302540.html. [Accessed November 2018].

[27] Hach, "Reagent set for silica, 1 - 100 mg / l SiO 2," 2017. [Online]. Available: https://nl.hach.com/reagentiaset-voor-silica-1-100-mg-l-sio-sub-2-sub/product-downloads?id=24929694814. [Accessed July 2018].

[28] H. Huiting, M. de Koning en E. Beerendonk, "Normalisatie van gegevens bij nanofiltratie en omgekeerde osmose," Kiwa N.V., Nieuwegein, 1999.

[29] J. Verdouw and H. Folmer, "Effect of water temperature on the normalized flux for RO-membranes," Kiwa N.V., 1999.

[30] Dow, "DOW FILMTEC™ Membranes - Handling, Preservation and Storage," Dow.

[31] M. T. Tognonvi, D. Massiot, A. Lecomte, S. Rossignol and J.-P. Bonnet, "Identification of solvated species present in concentrated and dilute sodium silicate solutions by combined Si NMR and SAXS studies," *Journal of Colloid and Interface Science,* pp. 309-315, 2010.

[32] E. Darton, "RO plant experiences with high silica waters in Canary Islands," *Desalination,* vol. 124, no. 1-3, pp. 33-41, 1999.

[33] S. S. Sablani, M. F. A. Goosen, R. Al-Belushi and M. Wilf, "Concentration polarization in ultrafiltration and reverse osmosis: a critical review," *Desalination,* no. 141, pp. 269-289, 2001.

Symbols & Abbreviations

A_{mem}	*Nominal active surface area*
CCD	*Closed-circuit desalination*
CF	*Concentration factor*
CT	*Cooling tube*
CP	*Circulation pump*
EC	*Electrical conductivity*
FP_1, FP_2	*Feed pumps*
GDP	*Gross domestic product*
ICP-AES	*Inductively coupled plasma atomic emission spectroscopy*
ICP-MS	*Inductively coupled plasma mass spectrometry*
J	*Flux through the membrane*
MTC	*Mass transfer coefficient*
n	*Experimentally-determined constant for calculation of $TCF_{\Delta P}$*
NDP	*Normalised driving pressure*
NPD	*Normalised pressure difference*
PD	*Pulse-dampener*
P_f, P_c, P_p	*Pressures of the feed, concentrate and permeate*
PV	*Pressure vessel*
$QCF_{\Delta P}$	*Correction factor for feed flow through the pressure vessel*
Q_f, $Q_{f,fresh}$, Q_p, Q_c	*Flow rates of feed, fresh feed, permeate, concentrate*
RO	*Reverse osmosis*
SM	*Static mixer*
TCF_{MTC}	*Temperature correction factor for MTC*
$TCF_{\Delta P}$	*Temperature correction factor for NPD*
TCF_{π}	*Temperature correction factor for osmotic pressure*
TDS	*Total dissolved salts*
T_f, T_{ref}	*Feed temperature, standard reference temperature*
TOC	*Total organic carbon*
t_{cycle}	*Cycle duration*

t_{ind}	*Nucleation induction time*
t_{res}	*System residence time*
U	*Membrane-dependent constant*
V_b	*Brine discharge valve*
$V_{circ.}$	*Circulation valve*
V_p	*Volume of permeate produced*
$V_{fl.}$	*Flushing inlet valve*
V_s	*Brine-sampling valve*
V_{sys}	*System volume*
$x_{EC \rightarrow TDS}$	*Conversion factor of EC to TDS*
$x_{TDS \rightarrow \pi}$	*Conversion factor of TDS to osmotic pressure*
$X_{SiO_2,initial}$, $X_{SiO_2,expected}$	*Initial and expected silica concentrations*
ΔP_a	*Actual pressure difference across the pressure vessel*
η_T	*Viscosity at temperature T*
π_f, π_c, π_p	*Osmotic pressures of the feed, concentrate and permeate*
γ_{sys}	*System recovery*

Appendices

A. Materials and Methodology

A.1. Specifications of the online meters used

Name	Manufacturer	Reading	Range	Accuracy
Feed Pressure meter	Gems Sensors & Controls	Absolute pressure	0 - 40 bars	0.25%
Conc. Pressure meter	Endress+Hauser	Gauge pressure	0 - 25 bars	-
Feed flow meter	Gems Sensors & Controls	Turbine flow meter	6 - 600 L/h	3%
Permeate flow meter	Gems Sensors & Controls	Turbine flow meter	6 - 150 L/h	3%
Digital Multiparameter meter	WTW	EC	0.01 - 2000 mS/cm	± 0.5%
		Temperature	0 to 100 °C	± 0.2 °C

A.2. Design of the static mixer (Primix)

Rev.:	Revision note:	Drawn date:	Checked date:	Approved date:

Tolerance for pressure vessels according DIN 28005-1

Range [mm]	Vessel length [mm]	Distance nozzle to reference line [mm]	Nozzle facing to reference line [mm]
>30 - 120	± 3	± 2	± 3
>120 - 400	± 4	± 2	± 4
>400 - 1000	± 6	± 3	± 6
>1000 - 2000	± 8	± 4	
>2000 - 4000	± 11	± 6	
>4000 - 8000	± 14	± 8	
>8000 - 12000	± 18	± 10	

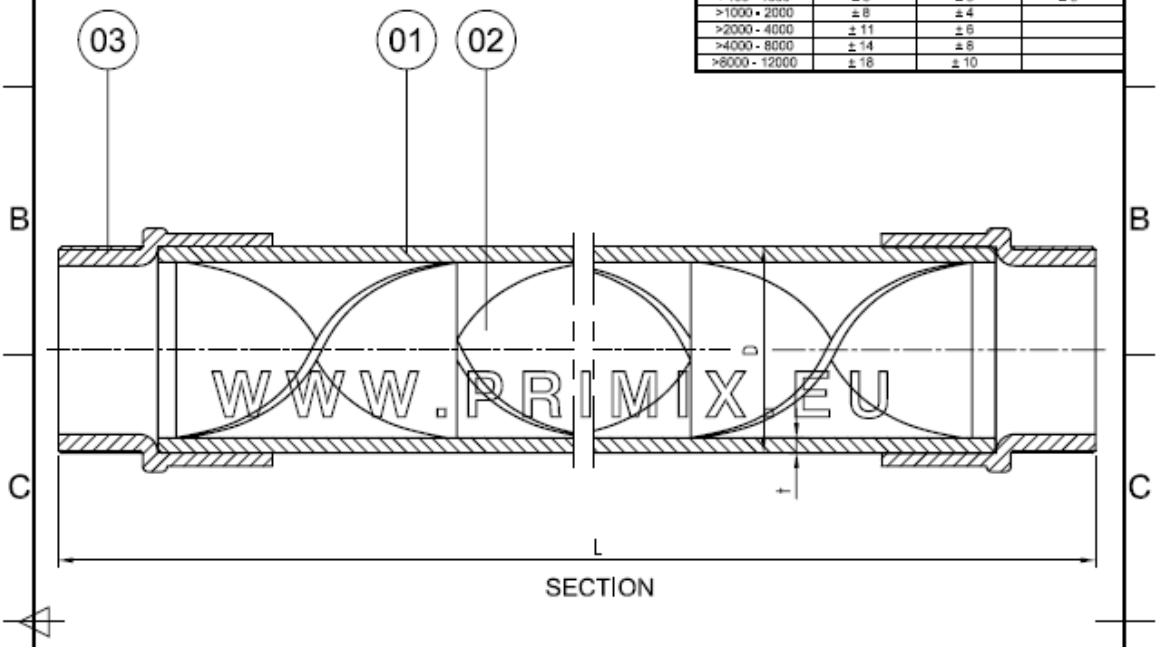

SECTION

MIXER DIMENSION & WEIGHT (BSP(M) nipples)

Size	Outside diameter	Wall thickness	NUMBER OF ELEMENTS 2		3		4		5		6	
	D [mm]	t [mm]	L [mm]	W [kg]	L [mm]	W [kg]	L [mm]	W [kg]	L [mm]	W [kg]	L [mm]	W [kg]
DN10 / 3/8"	16	1.2	100	0.04	121	0.04	143	0.04	164	0.04	186	0.05
DN15 / 1/2"	20	1.5	118	0.0	146	0.1	173	0.1	199	0.1	226	0.1
DN20 / 3/4"	25	1.9	134	0.1	168	0.1	202	0.1	235	0.1	269	0.1
DN25 / 1"	32	2.4	159	0.1	203	0.2	246	0.2	289	0.2	332	0.2
DN32 / 1 1/4"	40	3.0	187	0.2	241	0.3	296	0.3	349	0.4	403	0.4
DN40 / 1 1/2"	50	3.7	216	0.3	284	0.4	353	0.5	420	0.6	488	0.7
DN50 / 2"	63	4.7	258	0.6	343	0.8	429	0.9	520	1.1	606	1.2
DN65 / 2 1/2"	75	5.6	298	0.6	400	0.8	502	1.0	609	1.3	711	1.5
DN80 / 3"	90	6.7	347	1.1	469	1.6	592	2.1	719	2.6	842	3.1
DN100 / 4"	110	8.2	415	1.9	565	2.7	720	3.6	869	4.4	1019	5.3

Item No.:	Description:	Reference standard / drawing:	Material:	Mat. Cert.:	No.-off:	Final dimension	Weight:	Rev.:
03	Adaptor bush equal	PN16 (+GF+) BSP(M)	PVC-U		2			
02	Helical Shaped element		PVC-U					
01	Housing	SDR 13.5 PN16 (+GF+)	PVC-U		1			

Drawn by:	Checked by:	Approved by:	Date:	Client ref.:	Project:	Scale:	Format:
NR	RJW		10/05/05			1:~	A4

PRIMIX
Postbus 220, 3640 AE Mijdrecht
Nijverheidsweg 17-f, 3641 RP Mijdrecht
The Netherlands
T +31 (0)297-28 77 78
F +31 (0)297-28 60 30
E info@primix.eu
I www.primix.eu

Projection:

Title: QDS PVC BSP(M) STATIC MIXER

dwg.no.:	Sheet:	Rev.No.:
PMS___-___-PVC-BSP(M)	1/1	1

A.3. Sampling points for the membrane autopsy

The following figures show the positions of the coupons on the spread-out element.

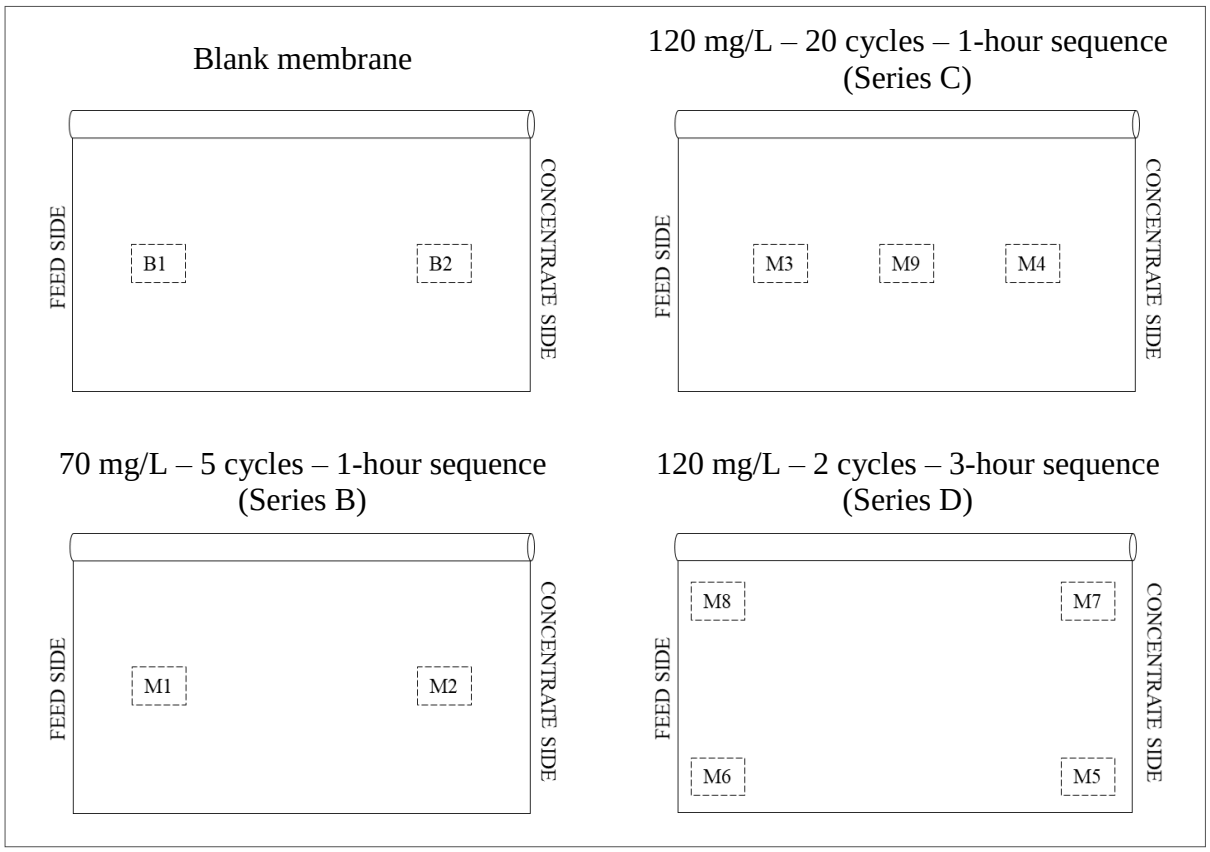

A.4. Derivation of the concentration factor formula

Mass balance of the system:

$$Feed = Permeate + Brine$$

$$V_f \cdot X_f = V_p \cdot X_p + V_b \cdot X_b \quad \text{(i)}$$

Where,

V_f, V_p and V_b are the volumes of total feed consumed, permeate produced and brine produced, respectively, in *L*; and

X_f, X_p and X_b are the concentrations of Na in the feed, permeate and brine (concentrate), respectively, in *mg/L*.

In terms of system recovery (γ_{sys}),

$$V_p = \gamma_{sys} \cdot V_f \;\; and \;\; V_b = \left(1 - \gamma_{sys}\right) \cdot V_f \quad \text{(ii)}$$

$$\gamma_{sys} = 1 - \frac{1}{CF} \quad \text{(iii)}$$

Substituting Equation (iii) in Equation (ii),

$$V_p = \left(1 - \frac{1}{CF}\right) \cdot V_f \;\; and \;\; V_b = \left(\frac{1}{CF}\right) \cdot V_f \quad \text{(iv)}$$

Substituting Equation (iv) in Equation (i),

$$V_f \cdot X_f = V_f \left\{\left(1 - \frac{1}{CF}\right) \cdot X_p + \frac{1}{CF} \cdot X_b\right\} \quad \text{(v)}$$

$$X_f = \frac{(CF - 1) \cdot X_p + X_b}{CF} \quad \text{(vi)}$$

$$CF \cdot \left(X_f - X_p\right) = X_b - X_p \quad \text{(vii)}$$

Therefore,

$$CF = \frac{X_b - X_p}{X_f - X_p} \quad \text{(viii)}$$

Since concentration of Na is linearly-related to the EC of each stream, Equation (viii) should be valid with the substitution of EC values of the respective flows.

$$CF = \frac{EC_c - EC_p}{EC_f - EC_p} \quad \text{(ix)}$$

Where, EC_f, EC_p and EC_c are the electrical conductivity of the feed, permeate and concentrate (brine), respectively, in µS/cm.

A.5. Derivation of the system volume formula

$$\gamma_{sys} = \frac{V_p}{V_f} \quad and \quad CF = \frac{1}{1-\gamma_{sys}} \tag{x}$$

Combining the above equations,

$$CF = \frac{V_f}{V_f - V_p} = \frac{V_f}{V_b} \tag{xi}$$

$$CF = \frac{V_p + V_b}{V_b}\ ; \qquad since\ V_f = V_p + V_b \tag{xii}$$

$$CF = \frac{Q_p \cdot t_{cycle} + V_{sys}}{V_{sys}}; \qquad since\ V_b = V_{sys} \tag{xiii}$$

$$V_{sys}(CF - 1) = Q_p * t_{cycle} \tag{xiv}$$

$$V_{sys} = \frac{Q_p \cdot t_{cycle}}{CF - 1} \tag{xv}$$

B. Results

B.1. Results of experiment series A: Initial experiments

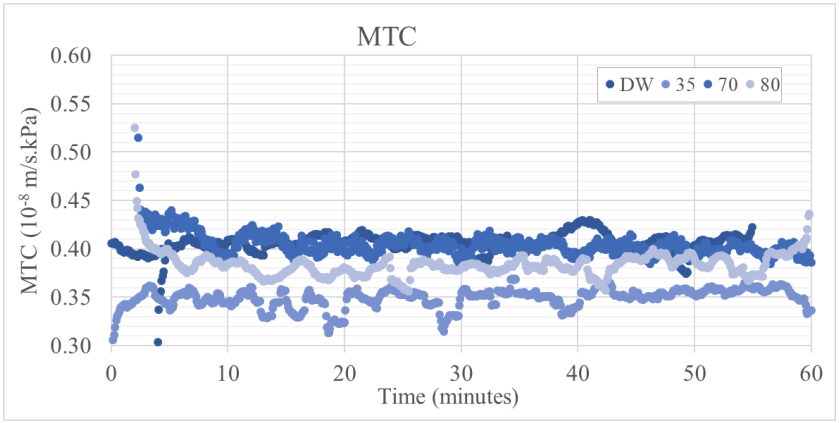

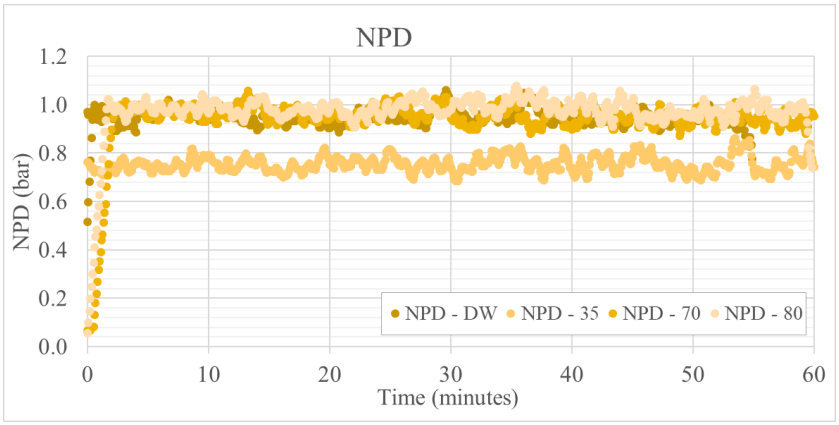

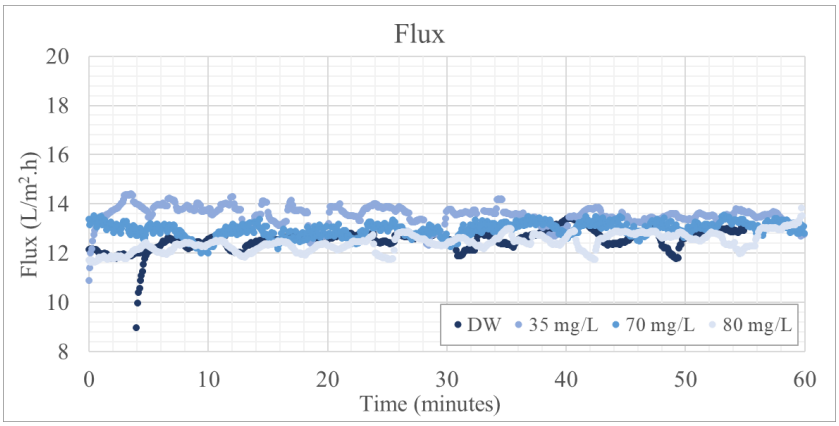

B.2. Results of experiment series B: 70 mg/L silica, 5 cycles of 1 hour

B.2.1. NPD graph for the 5 cycles of the 70 mg/L silica experiment

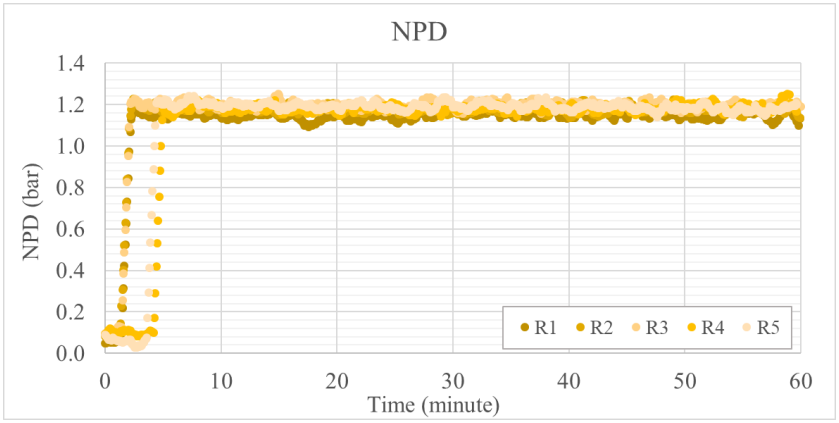

B.2.2. Flux graph for the 5 cycles of the 70 mg/L silica experiment

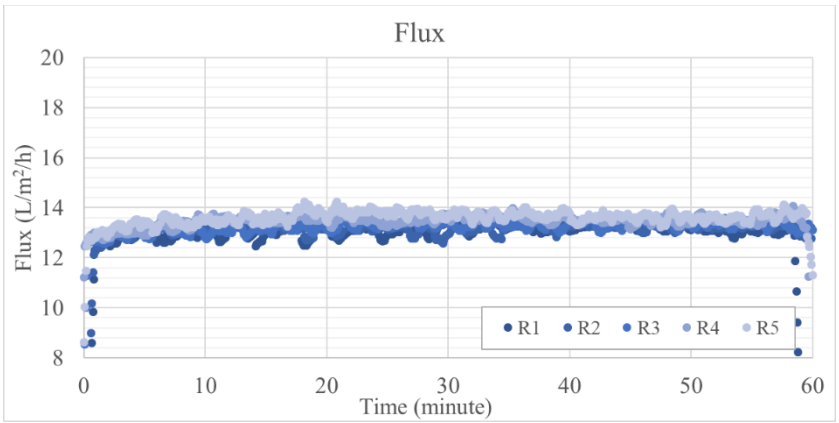

B.2.3. System recovery graph for the 5 cycles of the 70 mg/L silica experiment

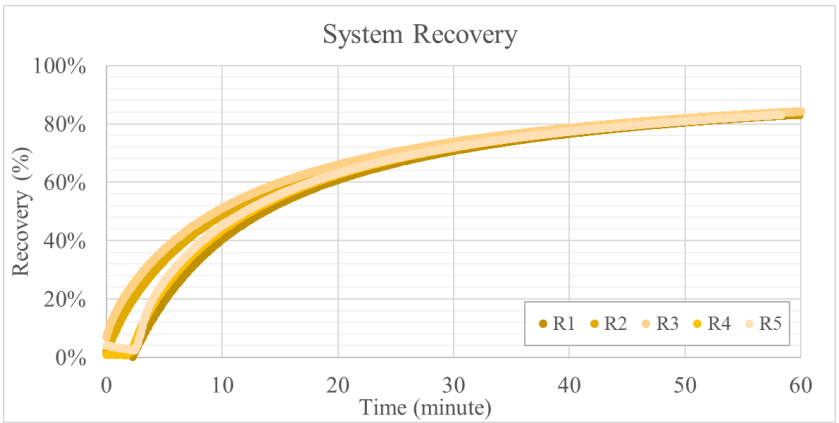

B.2.4. Feed and concentrate pressures for the 5 cycles of the 70 mg/L silica experiment

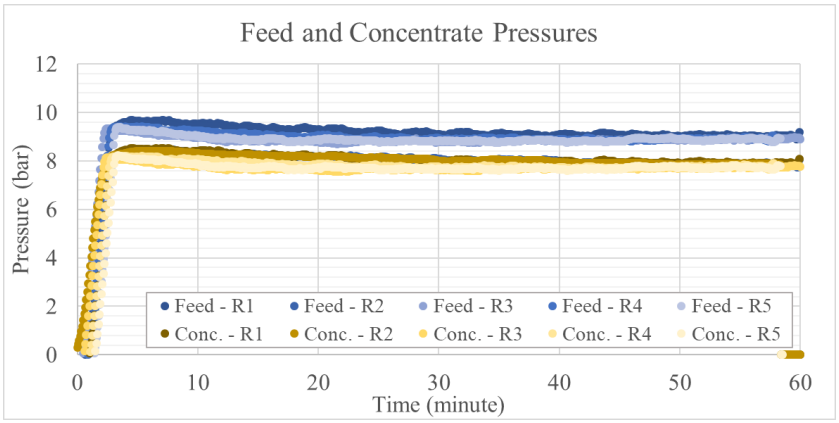

B.2.5. Average feed and concentrate temperature for the 5 cycles of the 70 mg/L silica experiment

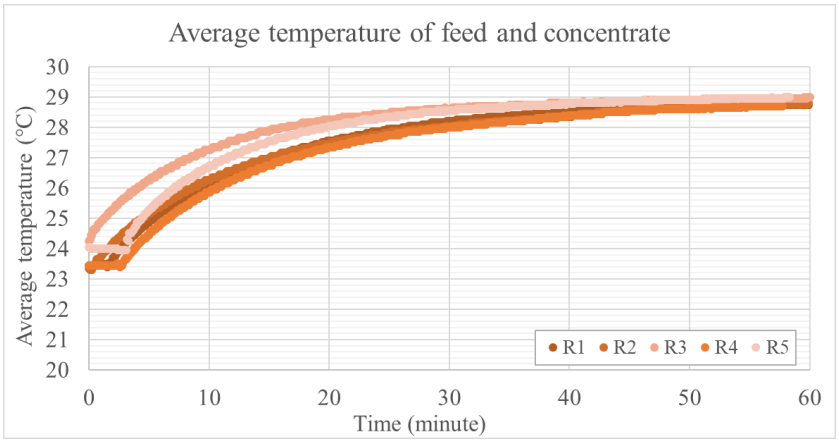

B.3. Results of experiment series C: 120 mg/L silica, 20 cycles of 1 hour

B.3.1. Flux and recovery for the 20 cycles of the 120 mg/L silica experiment

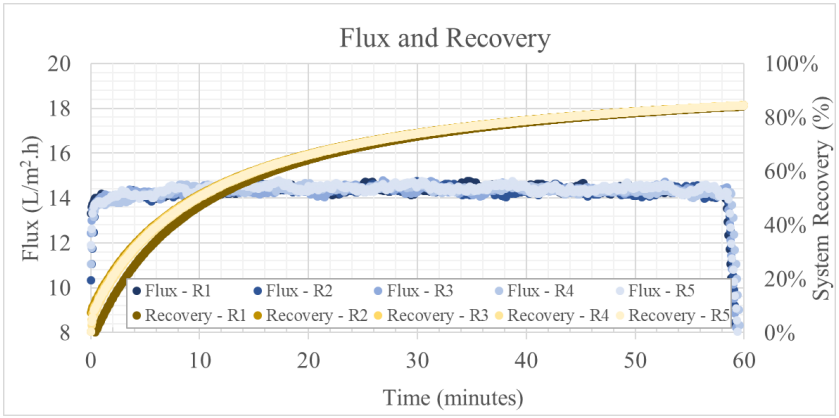

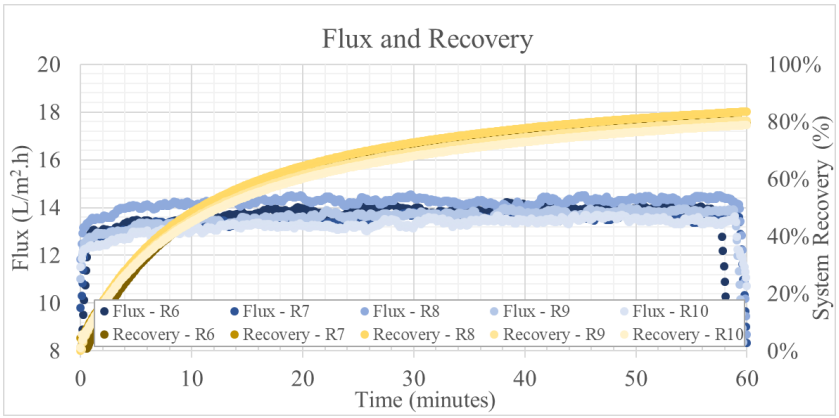

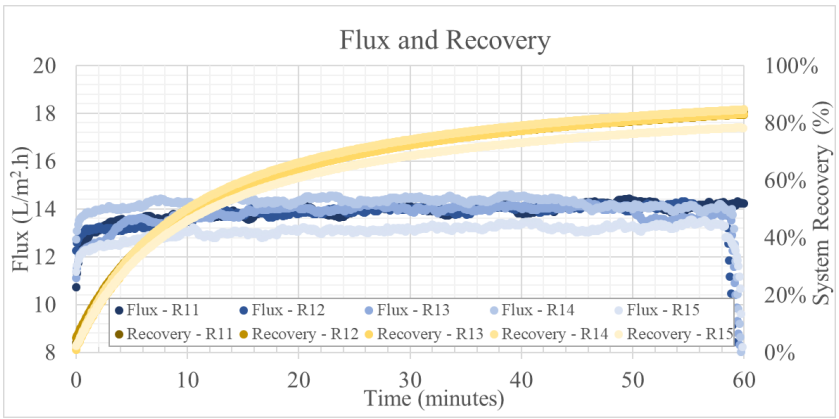

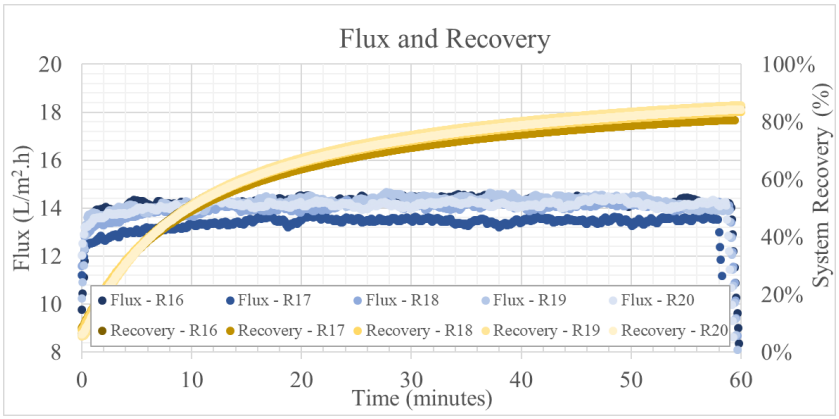

B.3.2. Feed and concentrate pressures for the 20 cycles of the 120 mg/L silica experiment

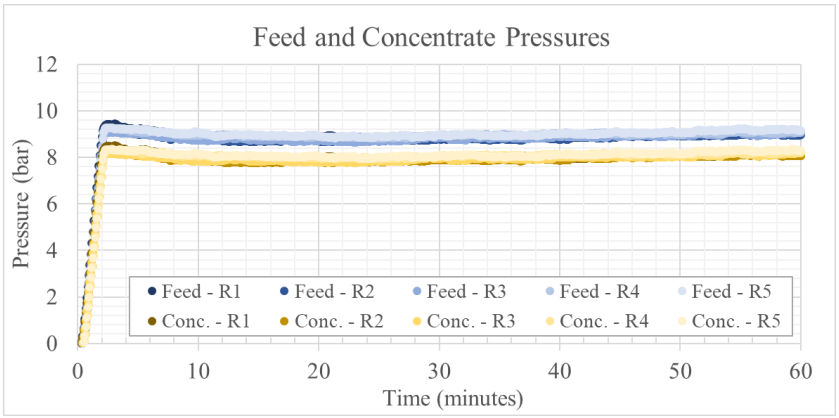

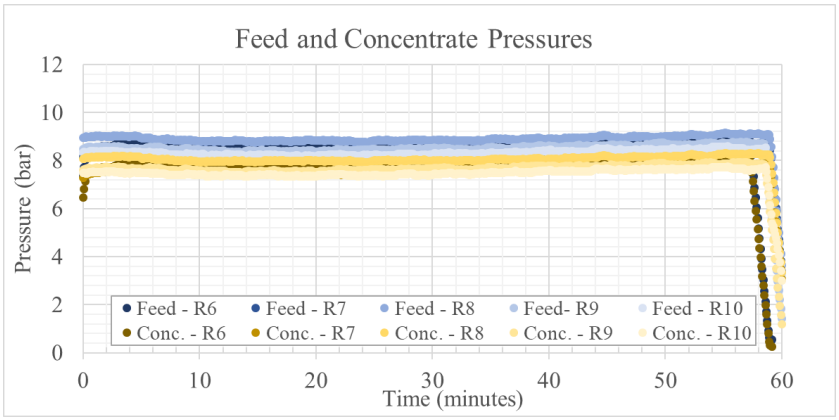

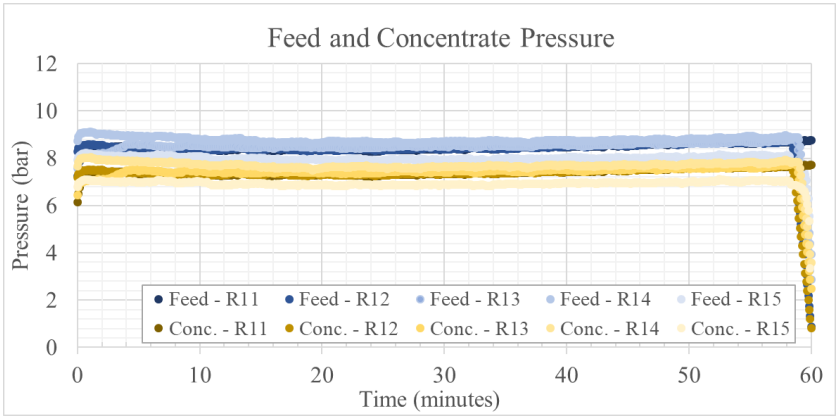

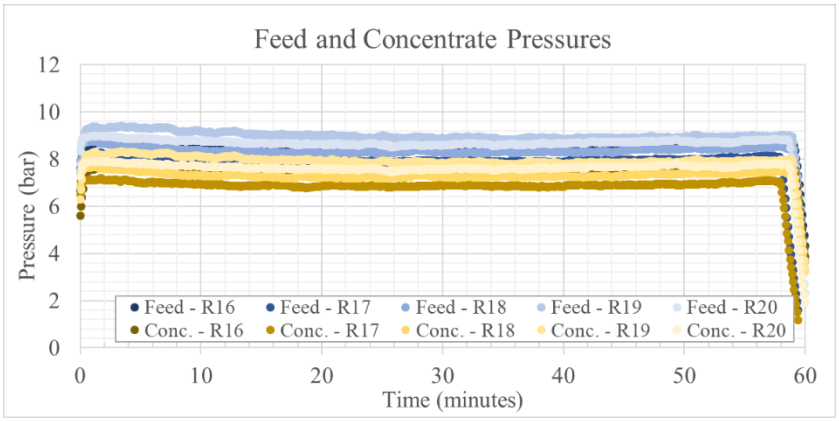

B.4. Results of experiment series D: 120 mg/L silica, 2 cycles of 3 hours

B.4.1. Variation of the EC in the 120 mg/L silica experiment, with 3-hour cycle duration

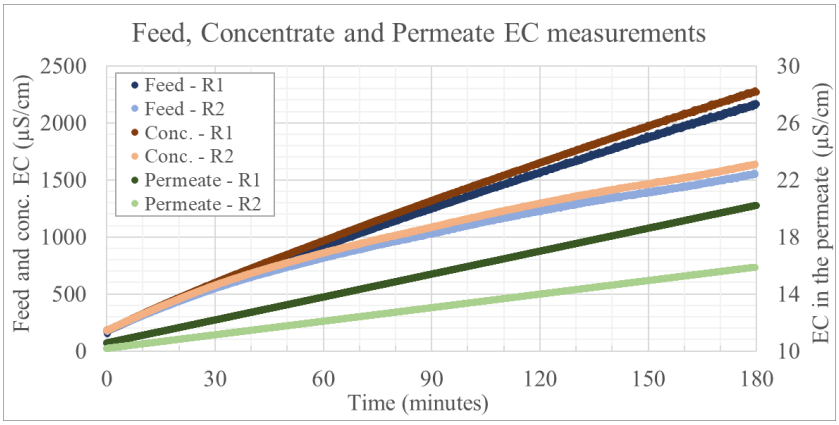

B.4.2. Flux and recovery for the 120 mg/L silica experiment, with 3-hour cycle duration

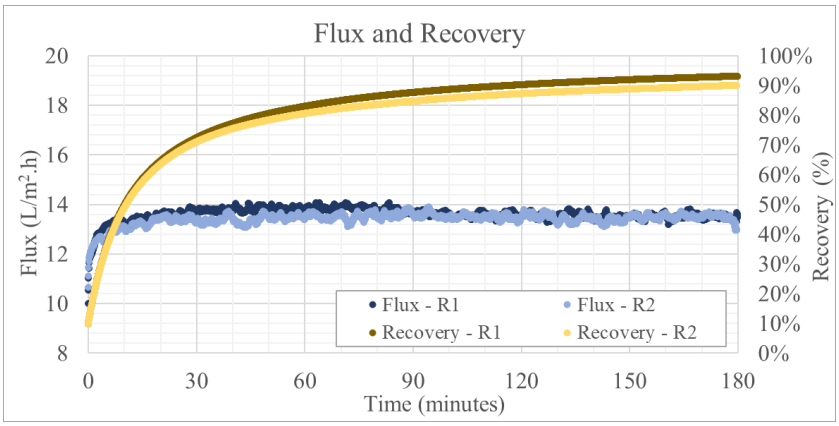

B.4.3. Feed and concentrate pressure for the 120 mg/L silica experiment, with 3-hour cycle duration